

**FAN mediates navigational capacity in leukocytes  
and tumour cells**

**I n a u g u r a l - D i s s e r t a t i o n**

zur

Erlangung des Doktorgrades

der Mathematisch-Naturwissenschaftlichen Fakultät

der Universität zu Köln

vorgelegt von

**Alexandra Böcke**

aus Bergisch Gladbach

Köln, 2012

---

Berichterstatter:

Prof. Dr. J. Howard

Prof. Dr. M. Krönke

Tag der mündlichen Prüfung: 25.06.2012

---

## Table of Contents

Abstract .....	5
Zusammenfassung .....	6
Abbreviations .....	8
1. Introduction .....	9
1.1 The TNF signalling pathway .....	9
1.2 Decision between life and death - a question of adaptor proteins .....	10
1.3 The adaptor protein FAN .....	13
1.4 The reorganisation of the actin cytoskeleton and cell migration .....	14
1.5 The zebrafish as a model .....	15
1.6 Aim of the study .....	16
2. Materials .....	17
2.1 Buffers .....	17
2.2 Primer and Oligonucleotides .....	18
2.3 Antibodies and reagents .....	19
3. Methods .....	20
3.1 Zebrafish methods .....	20
3.1.1 Keeping and raising zebrafish .....	20
3.1.2 Dechorionisation and storage of zebrafish embryos .....	21
3.1.3 In situ hybridisation of whole embryos .....	21
3.1.4 Injection of morpholino oligonucleotides into zebrafish embryos .....	23
3.1.5 Tail fin injury and confocal microscopy .....	23
3.1.6 Bacterial infection of the otic placode .....	24
3.1.7 Sudan Black Staining .....	24
3.2 Molecular biology methods .....	25
3.2.1 Polymerase chain reaction (PCR) .....	25
3.2.2 Agarose gel electrophoresis .....	26
3.2.3 Extraction of PCR fragments from agarose gels .....	26
3.2.4 Restriction enzyme digestion .....	26
3.2.5 Ligation .....	27
3.2.6 Transformation of bacterial cells .....	27
3.2.7 Growing <i>Escherichia coli</i> .....	27
3.2.8 Minipreparation of plasmid DNA .....	27
3.2.9 Midipreparation of plasmid DNA .....	27
3.2.10 Sequencing of DNA .....	28
3.2.11 In vitro transcription to produce <i>in situ</i> probes .....	28
3.2.12 Quantification of DNA by Spectrometric analysis .....	28
3.3 ShRNA and lentiviral gene transfer .....	29
3.4 Quantitative real-time PCR .....	29
3.5 Cell culture and transfection .....	30
3.6 Degradation assay .....	31
3.6.1 Gelatine labeling with Alexa Flour 594 .....	31
3.6.2 Generation of Alexa 594-gelatine coated cover slips .....	31
3.6.3 Growing cells on gelatine coated cover slips .....	31
3.6.4 Phalloidin staining of the cells .....	32
3.6.5 Confocal microscopy of B16 melanoma cells grown on cover slips .....	32
3.6.6 Quantification of the degradation of the extracellular matrix .....	32
3.7 Proliferation assay .....	32
3.8 Western Blot .....	33
3.8.1 Cell lysates .....	33

---

3.8.2	SDS polyacrylamid gelectrophoresis .....	33
3.8.3	Blotting and detection .....	33
3.9	Migration assay B16 mouse melanoma cells .....	33
3.10	Statistical analysis .....	33
4.	Results .....	34
4.1	FAN mediates navigational capacity of leukocytes responding to wounds and infection.....	34
4.1.1	Identification of zebrafish FAN .....	34
4.1.2	Morpholino knockdown in zebrafish embryos.....	37
4.1.3	FAN propels leukocytes motility during wound response .....	39
4.1.4	FAN is required for the oriented migration of leukocytes .....	41
4.1.5	FAN propels leukocytes motility during infection response.....	45
4.2	FAN has an impact on cell migration, proliferation and matrix degradation in melanoma cells <i>in vitro</i> .....	47
4.2.1	FAN knockdown in B16 mouse melanoma cells .....	47
4.2.2	FAN knock-down in B16 mouse melanoma cell lines results in impaired migration induction after TNF stimulation .....	49
4.2.3	The degradation of the extracellular matrix is reduced in FAN knock-down mouse melanoma cells .....	50
4.2.4	Mice injected with B16 mouse melanoma FAN knock-down cells display reduced tumour growth and metastasis .....	54
5.	Discussion .....	58
6.	References .....	64
	Erklärung.....	68
	Declaration of collaborators contributions.....	69
	Danksagungen .....	70
	Lebenslauf .....	71

## Abstract

FAN (factor associated with neutral sphingomyelinase activity) is an adaptor protein that specifically binds to the p55 receptor for TNF (TNF-RI). Previous investigations demonstrated that FAN plays a role in TNF-induced actin reorganisation by connecting the plasma membrane with actin cytoskeleton and FAN deficiency leads to an impaired migratory induction in MEF (mouse embryonic fibroblasts) cells and Langerhans cells after TNF stimulation suggesting that FAN may impact on cellular motility in response to TNF and in the context of immune inflammatory conditions. In this work the translucent zebrafish larvae was used for *in vivo* analysis of leukocyte migration after morpholino knockdown of FAN. FAN-deficient zebrafish leukocytes were impaired in their migration toward tail fin wounds leading to a reduced number of cells reaching the wound. Furthermore, FAN-deficient leukocytes show an impaired response to bacterial infections suggesting that FAN is generally required for the directed chemotactic response of immune cells independent of the nature of the stimulus. Cell-tracking analysis up to 3h after injury revealed that the reduced number of leukocytes is not due to a reduction in random motility or speed of movement. Leukocytes from FAN-deficient embryos protrude pseudopodia in all directions instead of having one clear leading edge. These results suggest that FAN-deficient leukocytes exhibit an impaired navigational capacity leading to a disrupted chemotactic response. Due to the involvement of FAN in the migratory behaviour in different cell types it is likely that FAN has a general role in the migration of cells. Another process, dependent on cell migration, is the metastasis of cancer cells. Cell migration of B16 mouse melanoma cells after TNF stimulation was reduced after FAN down-regulation. In addition, these cells displayed a reduced tumour growth and never developed metastasis after injection in the tail vein of wild-type mice.

## Zusammenfassung

FAN (factor associated with neutral sphingomyelinase activity) ist ein Adapterprotein, welches spezifisch die NSD Domäne des p55 TNF Rezeptors (TNF-RI) bindet. Vorangegangene Untersuchungen haben gezeigt, dass FAN durch die Verbindung der Plasma-Membran und dem Aktinzytoskelett, an der TNF induzierten Reorganisation des Aktinzytoskeletts beteiligt ist. Die Verbindung von Plasmamembran und Aktinzytoskelett erfolgt durch die Bindung von FAN an F-Aktin und PIP<sub>2</sub> (Phosphatidyl-Inositol4,5 Bisphosphat). Die Defizienz von FAN führt zu einer gestörten Zellmigration in MEF- (mouse embryonic fibroblasts) und Langerhans-Zellen nach der Stimulation mit TNF. Diese Beobachtungen haben zu der Annahme geführt, dass FAN eine Rolle bei der TNF induzierten Zellwanderung während immunologisch entzündlicher Prozesse hat.

In dieser Arbeit wurde der Zebrafisch als Modellorganismus benutzt um die Leukozytenwanderung zu Wunden zu beobachten. Der Zebrafisch eignet sich auf Grund der Transparenz der Embryonen und der dadurch ermöglichten *in vivo* Observation sehr gut als Modellorganismus. Darüber hinaus lassen sich dessen Proteine sehr leicht durch die Injektion von Morpholinos herunterregulieren. Um die Migration von Leukozyten zu untersuchen wurden den Embryonen Laserwunden an der Schwanzflosse beigebracht. Leukozyten, in denen FAN herunterreguliert ist, zeigen eine gestörte Wanderung zu einer Wunde. Diese Störung resultiert in einer verminderten Anzahl an Leukozyten an der Wunde. Zusätzlich zu der gestörten Wanderung zu Wunden zeigen FAN defiziente Leukozyten auch eine verminderte Wanderung zu Infektionen mit *E.coli* im optischen Tektum. Diese Ergebnisse implizieren eine allgemeine Notwendigkeit von FAN für die Wanderung von Immunzellen, die nicht stimulus- oder gewebeabhängig ist. Die Analyse der Zellwanderung bis zu drei Stunden nach Verletzung ergab, dass die Reduktion der Anzahl an Leukozyten nicht aus einer verminderten Wanderungsgeschwindigkeit der Leukozyten resultiert, sondern das Ergebnis des Verlusts der Direktionalität der Zellen ist. Anstelle der normalerweise von migrierenden Zellen gebildeten "leading edge", bilden FAN defiziente Leukozyten Pseudopodien in alle Richtungen und die Wahl der Migrationsrichtung scheint willkürlich zu erfolgen. Die Ergebnisse, die zeigen dass verschiedene Zelllinien einen Migrationsdefekt aufweisen wenn FAN fehlt, legt die Vermutung nahe, dass FAN ein wichtiger Faktor für koordinierte Zellmigration ist. Ein weiterer Prozess, für den die Wanderung von Zellen essentiell ist, ist die Metastasenbildung von Krebszellen. Um zu untersuchen, ob FAN auch einen Einfluss auf die Metastasierung von Krebszellen hat, wurden stabile B16 Mausmelanomzellen generiert, in

denen FAN durch lentivirale Transduktion herunterreguliert wurde. Diese Zelllinien zeigten ebenfalls eine verminderte Migration nach TNF Stimulation. Außerdem war das Tumorwachstum reduziert da diese Zellen weniger schnell proliferieren als die entsprechenden wildtypischen B16 Mausmelanomzellen. Nach Injektion der FAN-Knockdown-Mausmelanomzellen in die Schwanzvene von Wildtypmäusen konnten, im Gegensatz zu den Mäusen, die mit den wildtypischen Mausmelanomzellen injiziert wurden, keine Metastasen in der Lunge detektiert werden.

## Abbreviations

aa	amino acids
BEACH	beige and Chediak-Higashi
bp	basepairs
BSA	bovine serum albumin
C-terminal	carboxyterminal
DD	death domain
dpf	days postfertilization
<i>E.coli</i>	<i>Escherichia coli</i>
FAN/NSMAF	Factor associated with neutral sphingomyelinase activity
GFP	green fluorescent protein
hr	hour
HRP	horse radish peroxidase
IF	immunofluorescence
IB	immunoblot
kb	kilo base
kDa	kilo dalton
MEFs	mouse embryonic fibroblasts
min	minute
MO	morpholino oligonucleotide
NA	numerical aperture
NSD	nSMase activation domain
nSMase	neutral sphingomyelinase
N-terminal	aminoterminal
ORF	open reading frame
PBS	phosphate buffered saline
PCR	polymerase chain reaction
PFA	paraformaldehyd
rpm	rotations per minute
RT	room temperature
scr	scrambled
SDS	sodiumdodecylsulfat
SDS-PAGE	polyacrylamid gel electrophoresis
sek	second
TEMED	N,N,N',N'-tetramethyl diamine
Tris/HCl	tris[hydroxymethyl]aminoethane

## 1. Introduction

### 1.1 The TNF signalling pathway

The tumour necrosis factor (TNF), a pleiotropic cytokine, was initially identified as a factor that induces necrosis in tumour cells. Further studies identified TNF as a cytokine that acts as a major proinflammatory mediator and is involved in many biological processes like host defence against intracellular pathogens, wound healing and tumour defence (Locksley et al. 2001; Wajant et al. 2003). The TNF signalling pathway represents a double-edged sword. On the one hand TNF is a physiologically important cytokine, required for physiological responses, on the other hand the inappropriate expression is harmful and is implicated in a wide spectrum of human diseases like sepsis, diabetes, cancer, osteoporosis, multiple sclerosis, rheumatoid arthritis and inflammatory bowel disease (Aggarwal 2003; Chen and Goeddel 2002) making research on TNF signalling important for therapeutic approaches (Choo-Kang et al. 2005).

TNF is primarily produced by activated macrophages as a type II transmembrane protein arranged in stable homotrimers. The soluble homotrimeric TNF is released via proteolytic cleavage by the metalloprotease TNF alpha converting enzyme (TACE) (Wajant et al. 2003). Both forms, the membrane-embedded "pro" as well as the cleaved, soluble "mature" form are active as self-assembling non-covalent trimers that bind to the two TNF receptors, TNF-RI (CD120a) and TNF-RII (CD120b). The expression of TNF-RII is limited to cells of the immune system while TNF-RI is found on many different cell types, but receptor numbers on the cell surface vary (Pfeffer et al. 1993; Vandenabeele et al. 1995). TNF-RI is bound with a higher affinity than TNF-RII and most of the signalling pathways and subsequent biological effects are triggered by binding to TNF-RI (Hehlgans et al. 2002; Wiegmann et al. 1992). TNF-RI is involved in many diverse cellular processes like cell survival, proliferation, apoptosis and inflammatory responses mediated by the activation of kinases of the MAPK family, transcription factors like NF- $\kappa$ B, and caspases.

TNF-RI and TNF-RII belong to the TNF receptor superfamily. These TNFR-like receptors are type I transmembrane proteins that adopt elongated structures by a scaffold of disulfide bridges which form "cysteine-rich" domains (CRDs) that are the hallmark of the TNF superfamily (Locksley et al. 2001). None of the receptors of the mammalian TNF superfamily display any enzymatic activity. Signalling occurs by binding to one or more TNF-associated factors (TRAFs) (Aggarwal 2003).

## 1. Introduction

Despite the initial thought that receptor activation occurs via trimerisation after TNF binding, more recent studies revealed that the distal cyteine-rich domains mediate homophilic interaction of the receptor molecules in the absence of ligand. Binding of the TNF trimer leads to the release of the inhibitory protein silencer of death domains (SODD) from the intracellular domain of the receptor which allows conformational changes of the preformed receptor complex or resulting in the activation of the receptor complex and subsequent downstream signalling events (Chen and Goeddel 2002; Wajant et al. 2003).

### 1.2 Decision between life and death - a question of adaptor proteins

TNF simultaneously mediates apoptotic and anti-apoptotic or cell-survival signals. The initiation of the apoptotic caspase cascade does not require active protein synthesis, whereas anti-apoptotic signals do, and synthesis is mediated through the activation of NF- $\kappa$ B. Whether a cell undergoes apoptosis, survives or proliferates in response to TNF signalling depends on the balance between pro- and anti-apoptotic signals (Aggarwal 2003) (Fig. 1).

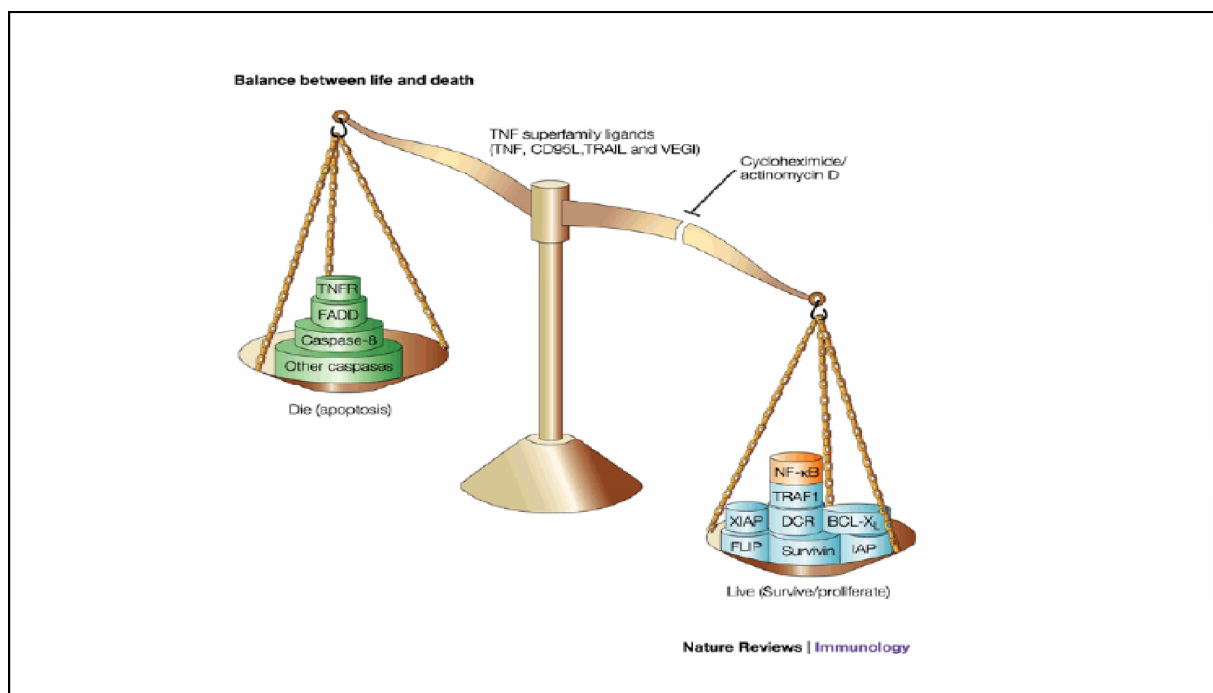


**Figure 1:** The composition and activation status of TNF receptor adapter proteins and additional downstream factors determines whether a cell will survive, undergo apoptosis or proliferate. From (Aggarwal 2003)

## 1. Introduction

---

The activation of different signalling cascades is mediated by the different adaptor proteins that bind to the intracellular domains of TNF-RI. After receptor complex activation the intracellular death domain of the TNF receptor complex is recognized by the TNF receptor-associated death domain (TRADD) adaptor protein. Binding of TRADD provides a scaffold for binding other adaptor proteins like receptor-interacting protein (RIP), TNF-R-associated factor 2 (TRAF2) and Fas-associated death domain (FADD). RIP, TRAF2 and FADD recruit key enzymes that are responsible for initiating signalling events (Chen et al. 2002).

Recruitment of TRAF2 and RIP to the TNF-RI leads to activation of the nuclear factor kappa B (NF- $\kappa$ B) pathway. In an un-induced state cellular I- $\kappa$ B proteins interact with the NF- $\kappa$ B dimers masking their nuclear localisation sequence and thus retaining the ternary complex in the cytosol. Binding of TRAF2 and RIP to the TNF-RI leads to the activation of the I- $\kappa$ B kinase (IKK) multiprotein complex (Perkins 2000). Activated IKK phosphorylates the regulatory domain of I- $\kappa$ B and marks it for proteasomal degradation, thus liberating NF- $\kappa$ B dimers for nuclear translocation where they act as transcription factor for a huge number of inflammatory-related genes.

TNF also mediates the activation of mitogen-activated protein kinases (MAPK) and the distantly related c-Jun N-terminal kinase (JNK) via TRAF2 recruitment. TRAF2 interacts with MAP kinase 7 (MKK7) which leads to the phosphorylation and activation of JNK. Upon activation, JNK translocates into the nucleus and enhances the transcriptional activity of transcription factors, for example, c-Jun and ATF2 by phosphorylation of their amino-terminal activation domains. c-Jun belongs to a group of basic region-leucine zipper proteins that dimerize to transcription factors, commonly designated as activator protein-1 (AP-1). The AP-1 proteins have an important role in cellular processes including proliferation, differentiation and induction as well as prevention of apoptosis (Wajant et al. 2003). The importance of JNK activation for TNF-mediated cellular responses is poorly understood. It has been reported that it is implicated in up-regulation of collagenases (Brenner et al. 1989), the chemoattractant MCP-1 (Hanazawa et al. 1993), E-selectin (Min et al. 1997) and in the regenerative response to liver injury (Brucoleri et al. 1997; Diehl et al. 1994).

TNF also activates the p38-MAPK signalling cascade. This requires the additional recruitment of RIP to TRAF2. The p38-MAPK signalling pathway is a mediator of inflammatory processes and activation leads to the up-regulation of IL-1 and IL-6.

TNF-RI, like other death domain containing receptors is able to induce apoptosis, but the TNF-RI mediated induction of apoptosis seems to have only a minor role *in vivo* compared to the regulation of inflammatory processes. Induction of apoptosis is inhibited by the activation

## 1. Introduction

of NF- $\kappa$ B. Mice deficient for components of NF- $\kappa$ B activation exhibit embryonic lethality (Yang et al. 2001). Thus, in contrast to Fas and TRAIL-R1/2 signalling where apoptosis is dominant over NF- $\kappa$ B activation, in TNF-R1 signalling NF- $\kappa$ B activation dominates over apoptosis-induction (Wajant et al. 2003). TNF-R1 mediated apoptosis is thought to proceed via recruitment of the adaptor protein Fas-associated death domain (FADD) and caspase-8. Two signalling complexes are involved in the apoptosis induction: the plasma membrane-bound complex I that contains TNF-R1, TRADD, TRAF2 and RIP and the cytosolic complex II that forms by the dissociation of TRADD and RIP from TNF-R1 and the association of TRADD and RIP with FADD and caspase-8 via their liberated death domains (Micheau and Tschopp 2003). The dissociation of the adapter complex from the receptor probably occurs after endocytosis of the receptor complex.

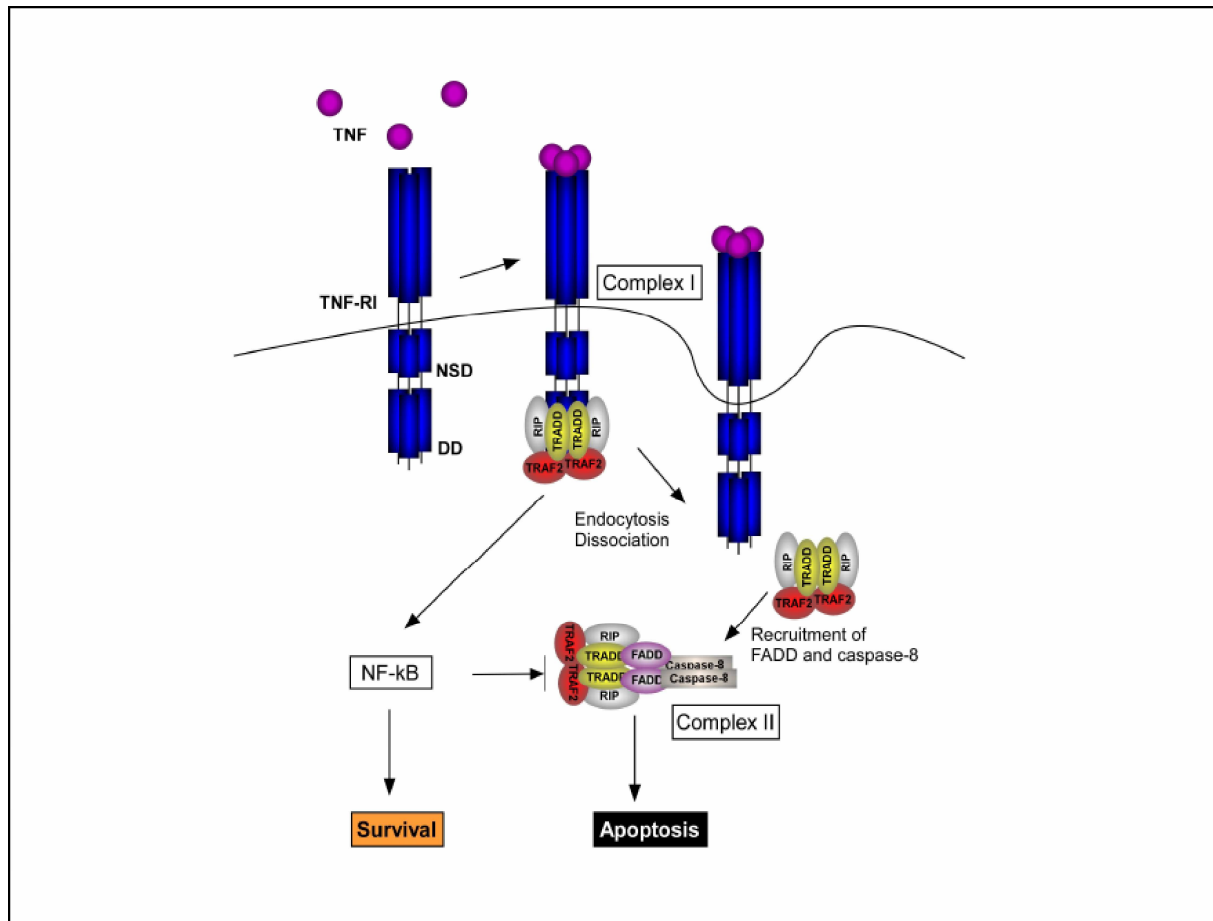


**Figure 2:** TNF-R1 signals via two complexes. After binding of TNF to TNF-R1, TRADD, RIP and TRAF2 are recruited. The membrane-bound complex I signals for NF- $\kappa$ B activation leading to inflammatory responses and cell survival, whereas complex II, which is formed after dissociation from the receptor and recruitment of FADD and caspase-8, induces apoptosis. (Dissertation Dirk Haubert).

### 1.3 The adaptor protein FAN

So far, nearly all functionally characterised adaptor proteins bind to the death domain (DD) of the TNF-RI receptor (Chen et al. 2002; Wajant et al. 2003). TNF-RI binds additional factors that may be important for TNF signalling (Adam-Klages et al. 1996; Boldin et al. 1995). The more membrane proximal neutral SMase (nSMase) activation domain (NSD) of TNF-RI has been recognised as a distinct functional domain for the activation of nSMase (Adam et al. 1996).

So far, only one protein, the adaptor protein FAN (factor associated with nSMase activity, also named NSMAF), binds to the NSD of TNFR-I (Adam-Klages et al. 1996). FAN belongs to the family of BEACH (beige and Chediak-Higashi) proteins. It is the smallest member of the BEACH protein family usually consisting of very large proteins with more than 2000 amino acid residues. Human FAN consists of 917 amino acids (aa), and FAN mRNA is expressed ubiquitously. At the C-terminal part FAN contains five WD-repeats that constitutively interact with the NSD domain of TNF-RI (Adam-Klages et al. 1996). The N-terminal part of FAN contains a weakly conserved PH and the BEACH domain. FAN is mainly located at the plasma membrane, which is due to an interaction of the PH domain with PIP<sub>2</sub> (Haubert et al. 2007). Biochemical studies and structural analysis suggested that the PH and BEACH domains interact to function as a single unit, which is essential for the activation of nSMase (Jogl et al. 2002).

Originally, FAN was identified as an adaptor protein that mediates TNF-induced activation of nSMase and it has been suggested that FAN plays an important role in the regulation of major inflammatory cellular responses to TNF (Adam-Klages et al. 1996).

The only obvious phenotype that could be observed in mice deficient for FAN was a delay in cutaneous barrier repair, suggesting a physiological role of FAN in epidermal barrier repair (Kreder et al. 1999).

Additionally, FAN has been implicated in TNF- and CD40-mediated induction of apoptosis (Segui et al. 1999; Segui et al. 2001), lysosomal permeabilization (Werneburg et al. 2004), IL-6 secretion (Malagarie-Cazenave et al. 2004), interaction with the WD protein RACK1 (Tcherkasowa et al. 2002) and regulation of cardiac cell death (O'Brien et al. 2003). Peppelenbosch et al, suggested the involvement of the membrane proximal region of TNF-RI in TNF-induced actin polymerization. Haubert et al. previously reported that mouse embryonic fibroblasts (MEFs) isolated from FAN<sup>-/-</sup> mice were impaired in TNF-induced actin reorganization. Mechanistically, FAN connects the plasma membrane with the cytoskeleton

## 1. Introduction

---

and mediates TNF-induced activation of the small GTPase Cdc42 and actin reorganization. Furthermore, FAN<sup>-/-</sup> MEFs are impaired in their motility in response to TNF *in vitro*, suggesting a role of FAN in cellular motility (Haubert et al. 2007).

### 1.4 The reorganisation of the actin cytoskeleton and cell migration

The actin cytoskeleton of a cell comprises a network of three types of protein filaments, actin, microtubules and intermediate filaments. The actin cytoskeleton is crucial for the generation and maintenance of cell morphology and polarity, in endocytosis, intracellular trafficking, in contractility, motility and cell division. (Winder and Ayscough 2005) Many of these processes depend on the ability of actin to rapidly polymerise and depolymerise as a results of the cell communication with the environment that leads to the constant reorganisation of the actin cytoskeleton. The assembly and disassembly of actin filaments and their organisation into higher-ordered networks is regulated by actin-binding proteins (ABPs) that are controlled by specific signalling pathways. In principle, actin exists in two forms, the globular monomeric (G) actin, a protein of 43 kDa, and the filamentous, polymeric (F) actin. Actin filaments are polar since all subunits face the same direction. Monomers add faster to one end, designated as the "barbed" or "plus" end than to the end designated as "pointed" or "minus" end. Polymerisation of actin filaments is mediated by ATP hydrolysis. *In vivo*, ABPs are crucial for rapid filament nucleation, because this is an energetically unfavourable process until a nucleus of three associating monomers is formed. After that, the addition of subsequent monomers at the barbed end is favourable and the filament elongates rapidly. New filaments can form de novo or from existing filaments.

For the form and function of cells, the organisation of actin into actin networks and higher-ordered structures is necessary. Higher-order F-actin structures are formed by two actin-binding activities: the bundling and cross-linking of F-actin (Winder and Ayscough 2005). Other ABPs do not affect the actin dynamics or actin structures but use actin as a scaffold, physical support or track. These ABPs are classified into three main categories: myosins that use actin as a track to move their specific cargo; anchors that connect actin to membranes or membrane proteins; and linkers between actin and other cytoskeletal elements for example cell adhesion receptors, microtubules and intermediate filaments.

One cellular process that requires the rapid reorganisation of the actin cytoskeleton is the directional motility of cells which is a fundamental cellular process essential for embryonic

## 1. Introduction

---

development, wound healing, immune responses and tissue development and also for the migration and metastasis of cancer cells. Four essential steps are involved in motility of cells: protrusion of the leading edge, adhesion to the substratum, retraction of the rear and de-adhesion (Pollard and Borisy 2003).

The structures forming the leading edge are lamellipodia. These are sites of rapid membrane protrusion and retraction and are composed of a dendritic actin network containing branched actin filaments, the Arp2/3 complex that mediates actin filament branching, capping proteins and cofilin. The lamellipodia exhibit rapid actin flow rates as well as a band of rapid polymerisation and depolymerisation parallel to the leading edge. This dendritic actin network terminates about 1 - 3  $\mu\text{m}$  from the leading edge, after which the lamellar network, that is composed of long actin filament bundles, rich in tropomyosin and myosin II and exhibits slower actin flow rates, predominates (Nicholson-Dykstra et al. 2005). The branching network at the leading edge induces a protrusion in the direction of motility. The induction of protrusions is regulated by small GTPases of the Rho family, namely Cdc42 and Rac. Local activation of Cdc42 and Rac enhances the activity of PI3K and the production of PI(3,4)P<sub>2</sub>/PIP<sub>3</sub> at the leading edge. PI3K in turn activates integrins and other adhesion molecules that stabilize the protrusion via structural connections to the actin filaments and in addition signal to Rac that promotes the recruitment of additional integrins and formation of adhesions. Adhesions transmit propulsive forces and serve as traction points over which the cell moves. Disassembly of adhesions and rear retraction complete the migration cycle (Ridley 2003).

### 1.5 The zebrafish as a model

The zebrafish, *Danio rerio*, is emerging as a powerful model organism to study the genetics underlying development, normal body function, and disease. The zebrafish combines a number of key embryological and experimental advantages. It is easy to maintain and breed and embryos can be easily manipulated by microinjection and cell transplantation. Another advantage of zebrafish embryos is their rapid development. Embryogenesis only takes about 24 hours and organogenesis is largely completed after 5 days (Dahm and Geisler 2006). Furthermore, the translucency in larval stages makes it amenable to live-imaging approaches. Initially, zebrafish research was centered on mutagenesis screens (forward genetics) but now also reverse genetic methods like morpholino knock-down and TILLING are well established.

## 1. Introduction

---

Morpholinos are oligonucleotides of 18 to 25 bases with a modified backbone: instead of the deoxyribose or ribose molecules, linking the bases, they contain morpholine rings and the ionic phosphate groups are replaced by non-ionic phosphodiamitates. These modifications make morpholinos inert for nuclease degradation resulting in a stable Morpholino-RNA-heteroduplex. The morpholino oligonucleotide binds sequence-specific to the targeted RNA. Generally, morpholinos can bind to the start codon (ATG) of a target mRNA preventing the formation of the translation machinery and thus, acting as a steric block. Another targeting strategy is the design of morpholinos that bind to a specific splicing site of the target RNA, binding of the morpholino masks the splicing site and this usually results in the loss of exons in the mature mRNA leading to frame-shifts and the generation of non-functional proteins. Morpholinos can be easily injected into the yolk of a one-cell stage embryo blocking the expression of the target gene for several days. The resulting effect of a morpholino injection is a phenotype that closely resembles or is identical to that of a loss-of-function mutant (Dahm and Geisler 2006).

### 1.6 Aim of the study

Reorganisation of the actin cytoskeleton plays a crucial role in the motility of cells. Cell motility is a fundamental cellular process essential for embryonic development, wound healing, immune responses and tissue development, but it also has an important role in cancer cell metastasis. Haubert et al revealed a role of FAN in cell migration *in vitro*. For this purpose the first aim of this work was to reveal whether FAN is also involved in cell migration *in vivo*. To investigate the impact of FAN on immune cell migration and motility live imaging studies in zebrafish embryos were performed. Zebrafish embryos were used to image the wound- and infection-triggered inflammatory response.

The second aim of this work was to demonstrate an involvement of FAN in metastasis and growth of tumour cells. To this end, B16 mouse melanoma cells were used and stable FAN knock-down mouse melanoma cell lines were generated. Migration assays were performed and the path length of knock-down cell lines was compared to that of wild-type cell lines. In addition to the ability to migrate, to metastasise, cells also need to gain the ability to degrade the extracellular matrix, thus, degradation assays were performed. To display the metastatic behaviour of FAN knock-down cell lines *in vivo*, mice were injected with B16 mouse melanoma cell lines.

## 2. Materials

### 2.1 Buffers

E3 buffer (60×stock, 2L)	34.4g NaCl, 1.52g KCl, 5.8g CaCl <sub>2</sub> *2H <sub>2</sub> O, 9.8g MgSO <sub>4</sub> *7H <sub>2</sub> O
LB Media (1L)	10g Tryptone, 5g Yeast extract, 5g NaCl, (pH 7),
50×TAE buffer (1L)	242g TrisBase, 57,1 mL acetic acid, 100 mL 0.5 M EDTA (pH 8,0)
6× DNA loading buffer	20% Ficoll-400, 0.025% Xylenecyanol, 0.025% brome phenol blue
Oligonucleotide annealing buffer	30 mM Hepes (pH 7,4), 100 mM KAc, 2 mM MgAc, 1 mM EDTA
<b>In situ hybridisation</b>	
Hyb+	50% Formamide, 5×SSC, 0.1% Tween 20, 1 mg/mL tRNA, 50µg/mL Heparin, adjust pH to 6.0 with citric acid
Hyb-	50% Formamide, 5×SSC, 0.1% Tween 20, adjust pH to 6.0 with citric acid
20×SSC	3 M NaCl, 0.3 M Trisodiumcitrate (pH 7)
Blocking solution	2% goat serum, 2 mg/mL BSA in PBT
AP solution	100 mM Tris pH 9.5, 50 mM MgCl <sub>2</sub> , 100 mM NaCl, 0.1% Tween 20 in H <sub>2</sub> O
Staining solution	135 µg/mL NBT, 105 µg/mL BCIP in AP solution
<b>Western blot</b>	
CHAPS lysis buffer	10 mM HEPES (pH 7.4), 150 mM NaCl, 1% CHAPS, complete protease inhibitor cocktail (Roche)
SDS sample buffer (5×)	25% glycerol, 0.6 M Tris-HCl, 144 mM SDS, 0.1% brome phenol blue
Blot transfer buffer	25 mM Tris-HCl, 190 mM glycine, 20% methanol
S-PBS	120 mM NaCl, 10 mM NaH <sub>2</sub> PO <sub>4</sub> , 30 mM K <sub>2</sub> HPO <sub>4</sub> pH 7.6
Blocking buffer	10 mM Tris-HCl, 150 mM NaCl, 5% milk powder, 2% BSA, 0.1% Tween-20, pH 7.4-7.6
SDS running buffer (1L)	190 mM glycine, 20 mM Tris-Base, 0.1% SDS

Table 1: Buffers

## 2. Materials

### 2.2 Primer and Oligonucleotides

<b>Primer for RT PCR</b>	<b>Sequence from 5' → 3'</b>
FAN forward RT	ATCTGGAAGTCGGTCTGGTG
FAN reverse RT	CCGTGTTACCGTCAGAACCT
GAPDH for RT	ACTCCACTCACGGCAAATTCA
GAPDH rev RT	CCTTCCACAATGCCAAAGTTG
<b>shRNA oligonucleotides</b>	
mFANsi1-sense	GATCCCCGGCTCCTTAAAGATATGTTTTCAAGAGA AACATATCTTTAAGGAGCCTTTTTA
mFANsi1-antisense	AGCTTAAAAAGGCTCCTTAAAGATATGTTTCTCTT GAAAACATATCTTTAAGGAGCCGGG
mFANsi2-sense	GATCCCCGGTTCCAAAGTGTTTCTGATTCAAGAGA TCAGAAACACTTTGGAACCTTTTTA
mFANsi2-antisense	AGCTTAAAAAGGTTCCAAAGTGTTTCTGATCTCTT GAATCAGAAACACTTTGGAACCGGG
<b>Primer for FANsh-construct sequencing</b>	
H1 min	AATATTTGCATGTCGCTATGTGTTCTG
super3'	AGGTCGACGGTATCGATAAG
<b>Primer for zebrafish FAN amplification</b>	
FAN for1	ATG GCT TTC ATC ACG AAG AAG
FAN for2	ACG CTA CAG AGA CAT GCC TG
FAN rev1	ACG CTA CAG AGA CAT GCC TG
FAN rev2	CAA GCA CAT TTT CTG CAG GA
FAN rev3	GCG GTC TGC TAA GTT GTT GA
β-Actin for	ATGGATGATGAAATTGCCGCAC
β-Actin rev	ACCATCACCAGAGTCCATCACG
<b>Primer for zebrafish FAN sequencing</b>	
FAN seq1	CTTTGAGTGGAATCTTTAAA
FAN seq2	CCACAAGATACCTGCTGCTC
FAN seq3	TTCAAAGAGCTGATTCCTGA
FAN seq4	GAAACACTTCTTTGTAGGCC
FAN seq5	CTACATTAA AGA TGT TCT CAA
FAN seq6	ATGTCTCTCCAATACTGTTG
FAN seq7	TCTGCTACATGGTTCTCGAG

## 2. Materials

---

<b>Morpholinos</b>	
FAN-E2I2	GTAAGCTGCTCACCTGTTTGTCTCG
FAN-I2E2	GCCATTGGTTCGCCTGTGTACAAAA
control Morpholino	CCTCTTACCTCAGTTACAATTTATA
<b>Primer for <i>in situ</i> probes</b>	
plastinT3for	AATTAACCCTCACTAAAGGGAGACGGCATC GGCT
plastinT7rev	TAATACGACTCACTATAGGGATCACCA GCGCATCC

Table 2: Primer and Oligonucleotides

### 2.3 Antibodies and reagents

All chemicals were purchased from Sigma (München, Germany) or Roth (Karlsruhe, Germany) unless indicated otherwise.

<b>Antibody</b>	<b>isotype</b>	<b>supplier</b>	<b>dilution</b>
anti-GFP	mouse monoclonal	Roche	1:1000
Anti-Digoxigenin-AP		Roche	1:5000
Phalloidin		Invitrogen	1:1000

Table 3: Antibodies

### **3. Methods**

#### **3.1 Zebrafish methods**

##### **3.1.1 Keeping and raising zebrafish**

###### **3.1.1.1 Growth conditions**

Starting with day 2, zebrafish were kept in an aquarium, consisting of several serial 12 L tank units, at a water temperature between 26 and 28 °C (Mullins et al. 1994). The maximum extent of utilization of a unit amounted to 40 fish per liter. The aquarium was supplied continuously with fresh water, whereby daily 1/10 of the liquid volume was replaced by fresh water. One half of the fresh water was adjusted by means of an ion exchange resin to a total hardness between 6-10 degrees of hardness units; the other half was transmitted from a reverse osmosis plant. Within the aquarium, the water was circulated by a pump system. Suspended particles were sieved by integrated filter units from the water and the filtered water was sterilized afterwards by UV irradiation. The accumulation of toxic substances (e.g. nitrite) was prevented by using a bacterial filter. Fish were fed thrice daily. Beside the usual fodder (Tetramin), Artemia and Bosmina were fed, in order to ensure balanced nutrition. The light and darkness rhythm was adjusted to 14 hours light and 10 hours darkness.

###### **3.1.1.2 Zebrafish embryos**

The collection of embryos for various experiments took place in the morning starting with the light phase. The evening before the adult male and female fish were put into a plastic box containing a sieve which lets the eggs pass through, preventing adult fish eating their own eggs. Male and female fish were divided by a separator. In the morning the divider was removed at the designated time point, allowing the fish to mate and 30 minutes later the embryos were collected. Embryos were kept in petridishes with E3 buffer before and after the experiments and were allowed to develop until the desired stage in an incubator at 28.5 °C.

#### **3.1.2 Dechorionisation and storage of zebrafish embryos**

##### **3.1.2.1 Mechanical dechorionisation of embryos**

Embryos of the desired growth stage were fixed in 4% Paraformaldehyd (PFA) in PBS (phosphate buffered saline). Embryos were fixed for two hours up to several days at room temperature (RT) or at 4 °C, respectively. After fixation embryos were transferred to PBST (PBS + 0.1 % Tween-20) and the chorion was removed using fine-pointed watch-makers forceps.

##### **3.1.2.2 Storage of embryos**

Embryos were stored in 4% PFA at 4 °C until they were used for further experiments.

#### **3.1.3 In situ hybridisation of whole embryos**

In situ hybridisation by means of Digoxigenin labelled probes is a non-radioactive procedure, which makes it possible, to determine the spatial expression of mRNA (Tautz et al. 1989). The embryos were incubated with digoxigenin labelled anti-sense RNA probes. The hybridised probes were then detected immunochemically, by means of alkaline phosphatase (AP) conjugated anti-digoxigenin Fab fragments, whereby the enzymatic conversion of specific substrates resulted in the production of colored precipitates.

In situ hybridisation of zebrafish embryos was performed as described in Schulte-Merker et al. (1992) with slight modifications:

Embryos were manually dechorinated and then fixed with PBS-based 4% PFA overnight at 4 °C.

Embryos were transferred to vials with 25%, 50%, 75% and 100% methanol in PBST, for 5 min, and subsequently stored in 100 % methanol at -20 °C until further treatment but at least overnight.

For rehydration, embryos were incubated for 5 min each in 100%, 75 %, 50% and 25 % methanol in PBST and then washed twice in PBST. Embryos were treated with proteinase K (10 mg/mL) for 8-12 min. The actual time of digestion was determined empirically; depending on the batch of enzyme used and on the embryonic stage. The proteinase K digestion was stopped with 4 % PFA and a second fixation with 4 % paraformaldehyde in PBS for 20 min was followed by four more washes with PBST for 5 min.

### 3. Methods

---

Subsequently embryos were prehybridised. For this purpose embryos were first incubated in a Hybridisation solution (Hyb+), for 1 hour at 65 °C. As much of the Hyb+ solution as possible was removed without allowing the embryos to come in contact with air. An equal volume of fresh Hyb+ containing 20 to 100 ng of digoxigenin labelled RNA probe was added to the tubes. After an overnight incubation at 65 °C the probe was removed followed by several washing steps:

100 % Hyb- at 65 °C for 15min

75 % Hyb- / 25 % 2× SSCT at 65 °C for 15 min

50 % Hyb- / 50 % 2× SSCT at 65 °C for 15 min

25 % Hyb- / 75 % 2× SSCT at 65 °C for 15 min

2× SSCT at 65 °C for 15 min

75 % 0.2×SSCT / 25 % PBST at RT for 15 min

50 % 0.2×SSCT / 50 % PBST at RT for 15 min

25 % 0.2×SSCT / 75 % PBST at RT for 15 min

PBST 2× at RT for 15 min

After these washing steps the embryos were incubated for 3h in Blocking solution. Blocking solution was replaced by an 1:5000 dilution of anti-Digoxigenin-AP F<sub>ab</sub> fragments (Roche) in Blocking solution. The incubation was carried out at 4 °C overnight, followed by six times washing for 15 min with PBST and two times washing in AP solution for 15 min. Detection was performed in AP-reaction buffer containing 135 µg/mL NBT and 105 µg/mL BCIP in the dark. The reaction was monitored under a binocular and stopped with 4 % PFA when the signal was satisfactory.

For analysis of the in situ hybridisation the embryos were transferred into 4 % methylcellulose (Sigma-Aldrich), on a hollow grinding slide and brought into a suitable position using a fine needle. The embryos were then analysed using a stereomicroscope (MZFLHIII; Leica) and photographed with a digital camera (Axiocam, Zeiss).

### 3. Methods

---

#### **3.1.4 Injection of morpholino oligonucleotides into zebrafish embryos**

##### **3.1.4.1 Morpholino design**

The appropriate sequences for morpholino design were selected from the full length sequences of FAN and sent to the company Gene tools for synthesis. The sequences of the morpholinos used in experiments are listed in table 2. Morpholinos were delivered lyophilised and were immediately diluted in H<sub>2</sub>O. The concentration of this stock solution was 3 mM.

##### **3.1.4.2 Injection of zebrafish embryos**

Zebrafish embryos were injected in the 1-2 cell stage into the yolk directly under the first cell(s). Embryos were put in a row on a agarose plate (1 % Agarose in E3 buffer), the water was removed and embryos were injected immediately using FemtoJet<sup>®</sup> and a Micromanipulator from Eppendorf. The injection solution consisted of 0.3 mM of each morpholino, 0.2 % Phenol Red and 0.1 M KCl of which, on average, 2 nl were injected per embryo.

The used capillaries (Hilgenberg) were pulled using a *Sutter P9 Micropipette Puller* (Sutter) (pulling conditions: heat 537, pull 100, velocity 100, time 150).

##### **3.1.5 Tail fin injury and confocal microscopy**

2-dpf tg (PU1-Gal4-UAS-GFP; MPX-GFP) (Peri et al. 2008; Renshaw et al. 2006) embryos either injected with control MO or FAN-MO were anaesthetised using tricaine (Sigma-Aldrich) according to standard protocols (Westerfield 1995) to prevent embryos from twitching. Embryos were embedded laterally in a small drop of 1.2 % low-melting agarose (Sigma-Aldrich) in a glass bottom culture dish (MatTek) for wounding of the fin and subsequent microscopy. Wounds at the end of the tail fin were made using a pulsed 532 nm cutting laser. Images were taken directly before injury and 1.5 hours after injury using an Olympus FV1000 confocal microscope and a 40× water objective. Leukocytes that reached a defined area after 1.5 h were counted and statistically analysed. For time-lapse microscopy Z-series were collected at 2.30 min and 4 min intervals for 3.15 hours. Projections of summed z-stacks, time-lapse animation and cell tracking were generated using Imaris (Bitplane).

To analyse leukocyte recruitment to the tail-fin wound each cell was tracked (using Imaris) from the point when it appeared until the end of the time-lapse series, or in case of the FAN-MO injected embryos, until it disappeared again. The average speed of leukocytes and their straightness, that means the ratio of netto length and the total length, were analysed by using

### 3. Methods

---

Imaris. The straightness is a coefficient between 0 and 1. A higher straightness indicates a more directed migration toward the wound.

The morphology of cells during their migratory route was captured from individual frames of time-lapse movies using Image J and tracing profiles were colour coded. These profiles outlined the protrusions extended by the cell and were subsequently analysed whether a cell had made the 'right' or the 'wrong' choice of pseudopodia. A 'right' choice of pseudopodia means that this pseudopodium is extended in the direction of movement. A 'wrong' choice means that a pseudopodium is extended against the direction of movement. This analysis was performed for 10 morphant and 10 control cells.

#### **3.1.6 Bacterial infection of the otic placode**

*E.coli* (DH5 $\alpha$ ) carrying the dsRed-expressing pGEMDs3 plasmid (Sieger et al. 2009; van der Sar et al. 2003) were grown in standard LB medium containing ampicillin (50  $\mu$ g/mL). For infections, a 3 mL overnight culture was centrifuged for 3 min at 4000 $\times$ g, supernatant was removed, and the pellet was washed three times with PBS. After washing, the pellet was resuspended in 500  $\mu$ L PBS. The final injection solution contained the washed *E.coli* diluted in PBS containing 1/10 Phenol Red.

2-dpf tg(PU1-Gal4-UAS-GFP) embryos either injected with a control MO or FAN-MO were anaesthetised using tricaine (Sigma-Aldrich) and arranged on agarose plates for infection. Infection was achieved by injecting the bacteria into the otic placode by using an Eppendorf Femtojet and micromanipulator. After infection embryos were embedded laterally in a small drop of 1.2 % low-melting agarose (Sigma-Aldrich) in a glass bottom culture dish (MatTek). Confocal microscopy was performed by using an Olympus FV1000 confocal microscope and a 40 $\times$  water objective. Images were taken 30 min after infection. Leukocytes that reached the side of infection after 30 min were counted and statistically analysed.

#### **3.1.7 Sudan Black Staining**

Sudan Black stains lipids and more intensely and irreversibly the granules of granulocytes. After washing with 70 % ethanol only the staining of granulocytes remains and therefore it is a suitable method to stain neutrophils. 2-dpf tg(PU1-Gal4-UAS-GFP) embryos either injected with FAN-MO or not injected were injured with a scalpel and fixed in 4 % PFA for 2 hours at RT. Embryos were washed three times with PBST. Next, embryos were incubated in 35 % ethanol/ 65 % PBST and 70 % ethanol, each for 5 min. Afterwards embryos were transferred to a 0.18 % sudan black staining solution (Sigma-Aldrich 380B) and incubated for 20 min

### 3. Methods

---

followed by two short washing steps in 70 % ethanol before they were progressively rehydrated. Subsequently PBST was replaced by a 30 % glycerol solution. This step was repeated with a 60 % and 90 % glycerol solution.

For analysis of the sudan black staining the embryos were transferred in 90 % glycerol solution on a hollow grinding slide and brought into a suitable position using a fine needle. The embryos were then analysed using a stereomicroscope (SMZ1500; Nikon) and photographed with a digital camera (DSFI1, Nikon).

## 3.2 Molecular biology methods

### 3.2.1 Polymerase chain reaction (PCR)

The polymerase chain reaction was performed after the method of Mullis et al. (1986).

#### 3.2.1.2 PCR with double stranded (ds) DNA as template

For the PCR reaction the T3 Thermocycler (Biometra) was used. The reaction was performed in a total volume of 50  $\mu$ L. For one reaction ~100 ng template DNA, 10 pM forward and reverse primer, respectively, and 25  $\mu$ L High Fidelity PCR Master mix (Roche) (containing enzyme, 2 $\times$  reaction buffer with 3 mM MgCl<sub>2</sub>) and nucleotides (dATP, dCTP, dGTP, dTTP, each 0.4 mM) were used. For the final volume of 50  $\mu$ L PCR grade water was added.

PCR conditions:

- (1) 98 °C  $\rightarrow \infty$
- (2) 98 °C  $\rightarrow$  30 min for denaturation
- (3) 98 °C  $\rightarrow$  10 sec
- (4) 55 - 65 °C  $\rightarrow$  1 min for primer annealing (temperature depends on the primers used)
- (5) 72 °C  $\rightarrow$  1 min for DNA synthesis (time depending on product length)
- (6) 29 repeats of steps 3 - 5
- (7) 72 °C  $\rightarrow$  7 min elongation
- (8) 8 °C  $\rightarrow \infty$

### 3. Methods

---

#### **3.2.1.3 PCR with first strand synthesis as template**

RNA from zebrafish embryos was isolated from embryos at different stages of development using the  $\mu$ MACS mRNA isolation kit (Miltenyi Biotec), according to the manufacturer's protocol, by addition of a DNaseI digest for 7 min to remove traces of genomic DNA. First-strand synthesis was performed by utilizing the Superscript III system (Invitrogen) using 300 ng of mRNA and random hexamer primers. For RT-PCR, 7.5 ng first-strand synthesis and RedTaq DNA polymerase (Sigma-Aldrich) were used. RT-PCR was performed as follows:

2 min at 94 °C

15 ( $\beta$ -actin) and 30 (FAN) cycles

94 °C for 15 sec

55 °C for 30 sec

72 °C for 1 min

7 min at 72 °C

For the amplification of FAN the primers Fan-for1 and Fan-rev1 were used. For the amplification of  $\beta$ -actin the primers  $\beta$ -actin-for and  $\beta$ -actin-rev were used.

#### **3.2.2 Agarose gel electrophoresis**

To separate nucleic acids depending on their size agarose gels were used. The amount of agarose was between 0.8 % und 2 % in 1  $\times$  Tris-Acetate Electrophoresis (TAE)-buffer. 1/6 6  $\times$  loading-buffer was added to the samples and the gel was run in a horizontal flat bed gel chamber filled with 1  $\times$  TAE. To visualize nucleic acids Ethidiumbromide was added to the melted gel (4 $\mu$ l Ethidiumbromide-solution (10 $\mu$ g/ml) in 100 mL) and the gels were analysed and pictured on a UV-Transilluminator (Biozym).

#### **3.2.3 Extraction of PCR fragments from agarose gels**

The fragment of interest was cut from the gel using a scalpel and transferred into a 1.5 mL eppendorf. The further extraction was done using the NucleoSpinExtractII Kit (Macherey-Nagel) according to the manufacturer's protocol.

#### **3.2.4 Restriction enzyme digestion**

The total volume of the reaction was 50  $\mu$ L. Depending on the following experiment 1-5  $\mu$ g of DNA were digested. Furthermore the reaction consisted of 1/10 reaction buffer and 10U of the desired restriction enzyme and was incubated for 1-2 hours at 37 °C. Afterwards the DNA was cleaned up by gel extraction (3.2.3).

### 3. Methods

---

#### **3.2.5 Ligation**

50 ng of the vector were used for the ligation and the amount of the insert-DNA was adjusted to a molar ratio of 3:1 to the vector in a total volume of 20  $\mu$ L. Additionally the ligation reaction contained 1 $\times$  rapid ligation buffer, 5U T4 DNA Ligase enzyme and autoclaved water. The reaction was incubated for 30 min at room temperature. The product of the ligation was then transformed into competent bacteria.

#### **3.2.6 Transformation of bacterial cells**

Plasmid DNA was transformed into competent *E.coli* and cultured overnight in LB Media at 37 °C. Selection was done with the accordant antibiotic:

Ampicillin: 150  $\mu$ g/mL

Kanamycin: 30 $\mu$ g/mL

#### Transformation of plasmid DNA:

1 ng of plasmid DNA was incubated on ice for 20 min with 100  $\mu$ L of competent bacteria followed by a heat shock for 1.5 min at 42 °C in a water bath. After this bacteria were incubated on ice for 3 min. For the expression of the marker of resistance 400  $\mu$ L LB Media were added and bacteria were incubated for 1 hour at 250 rpm at 37 °C. The transformed bacteria were plated on LB plates carrying the accordant antibioticum. Agar plates were incubated at 37 °C overnight.

#### **3.2.7 Growing *Escherichia coli***

*E. coli* were grown according to existing protocols (Sambrook et al., 1989).

#### **3.2.8 Minipreparation of plasmid DNA**

Using sterile tips single clones were picked from the bacteria plate and transferred to 5 mL LB-medium containing the required antibiotic. The culture was incubated overnight at 37 °C, 250 rpm. The next morning the plasmid preparation was performed using the NucleoSpin<sup>®</sup> Plasmid Kit (Macherey-Nagel) according to the manufacturer's protocol.

#### **3.2.9 Midipreparation of plasmid DNA**

100  $\mu$ L of the culture for the Minipreparation was given to 100 mL LB-medium containing the required antibiotic. The culture was incubated overnight at 37 °C, 250 rpm. The next morning the plasmid preparation was performed using the NucleoBond<sup>®</sup> Xtra Midi Kit (Macherey-Nagel) according to the manufacturer's protocol.

### 3. Methods

---

#### **3.2.10 Sequencing of DNA**

DNA sequencing was done by GATC Biotech. 20  $\mu\text{L}$  of the Template (containing 20 - 100 ng) and 20  $\mu\text{L}$  of the sequencing primer (10 pmol) were sent to GATC Biotech.

#### **3.2.11 In vitro transcription to produce *in situ* probes**

To produce labelled RNA probes the T3 or T7 polymerase (Roche) were used, depending on the promotor present on the template DNA. The probes were labelled using the Digoxigenin-RNA Labeling Mix from Roche.

The transcription reaction contained 200-500 ng DNA, 1 $\mu\text{L}$  10 $\times$  Labeling Mix, 1 $\mu\text{L}$  RNA Polymerase (20 U/ $\mu\text{L}$ ), 1  $\mu\text{L}$  10 $\times$  Transcription-buffer (contains 60 mM  $\text{MgCl}_2$ ) and 0.5  $\mu\text{L}$  RNase Inhibitor (40 U/ $\mu\text{L}$ , Roche, Mannheim). The total volume was adjusted to 10  $\mu\text{L}$  with  $\text{H}_2\text{O}_{\text{DEPC}}$  (DEPC = Diethylpyrocarbonat). The reaction was incubated at 37  $^\circ\text{C}$  for 2 hours and subsequently stopped by adding 1  $\mu\text{L}$  RNase free 0,2M EDTA. Purification of the transcripts was done by ethanol precipitation according to Roche protocol. The RNA pellet was resolved in a mixture of 20 $\mu\text{l}$   $\text{H}_2\text{O}_{\text{DEPC}}$  and 20  $\mu\text{L}$  Formamide and stored at -20  $^\circ\text{C}$ .

#### **3.2.12 Quantification of DNA by Spectrometric analysis**

To quantify the amount of DNA a Nanodrop photometer (GE Healthcare) was used. Reading was taken at a wavelength of 260/280 nm according to the manual.

#### 3.3 ShRNA and lentiviral gene transfer

To silence FAN expression, pENTR constructs were generated with a pair of oligonucleotides derived from FAN. Two shRNA sequences were designed to down-regulate FAN. For each shRNA construct two oligonucleotides containing 60 nucleotides (nt) were designed. After intermolecular hybridisation these oligonucleotides form an inverted repeat of 19 nt that is flanked by a 9 nt spacer. In addition the oligonucleotides contain the nucleotides necessary for the start and stop of polymerase III and unpaired ends for the cloning in the *Bgl II* and *Hind III* restriction sites of the pENTR vector. The upstream part of the inverted repeats corresponds to the target sequence of the target mRNA (sense strand), the downstream part of the inverted repeat is complementary to the target sequence (anti-sense strand).

The pENTR/FANshRNA constructs were transiently transfected into HEK293 FT cells cotransfected with FAN-GFP. The efficiency of shRNA knockdown was determined using western blot analysis. After confirming that both pENTR/FANshRNA constructs are functional they were stably expressed in cell lines using lentiviral gene transfer.

Starting with the pENTR clones, the pLenti6/V5DEST-GFP FANshRNA-, or scrshRNA-expressing vectors were created using LR recombination. The viral particles were produced according to manufacturer's instructions (ViraPower Lentiviral expression system; Invitrogen).  $2 \times 10^5$  B16 melanoma cells (B16 F1 and B16 F10) were transduced with the produced viral particles and stable cell lines were generated by blasticidin (Invitrogen) selection.

#### 3.4 Quantitative real-time PCR

Real-time RT-PCR is a highly sensitive method that allows the quantification of changes in gene expression. For the relative quantification of the expression of a target gene the expression of the target gene is related to the expression of a "Housekeeping Gene" (reference gene) which is a ubiquitous and homogeneously expressed gene like glyceraldehyde-3-phosphate dehydrogenase (GAPDH). The quantification extent of the mRNA starting amount is the so called Crossing Point (CP). The CP describes the number of cycles that are necessary to reach a constant defined level of fluorescence. The relative expression of the target gene in treated samples or after gene silencing is related to a Control (Ctrl), for example untreated samples or wild type expression. This is the  $\Delta\Delta\text{CP}$  method of quantification. In this method the a ratio is calculated that expressed the relative change of target gene expression between

### 3. Methods

---

treated samples and control samples that is normalised to a reference gene and in relation to the control. The ratio is determined as described below:

$$\Delta CP = CP(\text{target gene}) - CP(\text{reference gene})$$

$$\Delta\Delta CP = \Delta CP - \Delta CP(\text{Ctrl})$$

$$\text{ratio} = 2^{-\Delta\Delta CP}$$

Quantitative real-time PCR and the  $\Delta\Delta CP$  method of quantification was used to verify FAN knockdown in the putative knockdown cell lines generated with lentiviral gene transfer (see 3.3). To this end, CHAPS cell lysates from B16 F1 wt, B16 F10 wt and the putative cell lines were prepared as described in section 3.8.1, RNA was extracted from lysates using the NucleoTrap mRNA Kit (Macherey-Nagel Düren) according to the manufacturer's protocol. RNA was reverse transcribed into cDNA using the RevertAid™ First Strand cDNA Synthesis Kit (Fermentas) according to the manufacturer's protocol. The synthesised cDNA was used for real-time PCR reactions using an IQ5 thermal cycler (BioRad) and SYBR®-Green I chemistry and the following PCR program:

Cycle	Repeats	Step	Time	Temperature	PCR/Melt Data Acquisition	Temp. Change	End Temp.
1	1						
		1	3min	95 °C			
2	40						
		1	15 sec	95 °C			
		2	1 min	60 °C			
		3	1 min	72 °C	Real time		
3	81						
		1	30 sec	55 °C	Melt curve	0.5 °C	95 °C
4	1						
		1	∞	25 °C			

#### 3.5 Cell culture and transfection

B16 mouse melanoma cells (B16 F1 wt and B16 F10 wt) were cultured at 37 °C in DMEM (Biochrom, Berlin, Germany) and 10 % fetal bovine serum (FCS). B16 F1 knockdown and scrambled cell lines were cultured at 37 °C in DMEM/ 10 % FCS supplemented with 2 mM non-essential amino acids and 10 mM sodium pyruvate (Biochrom) and 12 µg/mL Blasticidin. B16 F10 knockdown and scrambled cell lines were cultured at 37 °C in DMEM/ 10 % FCS supplemented with 2 mM non-essential amino acids and 10 mM sodium pyruvate

### 3. Methods

---

(Biochrom) and 17 µg/mL Blastocidin. Blastocidin concentrations essential for each cell line were determined by titration.

HEK 293FT cells were cultured in DMEM / 10 % fetal bovine serum.

Cells were transfected using the calcium phosphate method (HEK 293FT) (Wigler et al. 1978).

## **3.6 Degradation assay**

### **3.6.1 Gelatine labeling with Alexa Fluor 594**

The labeling of gelatine with AlexaFluor 594 was performed using the AlexaFluor<sup>®</sup> 594 Protein Labeling Kit (Invitrogen) according to the manufacturer's protocol.

### **3.6.2 Generation of Alexa 594-gelatine coated cover slips**

15 mm cover slips were coated with gelatine conjugated to an Alexa 594 fluorophore. First, cover slips were sterilised with 70 % ethanol. The sterile cover slips were put on a drop (20 µL) of AlexaFluor 594-gelatine. Excess gelatine was removed with a pipette by tilting the cover slip. The coated site of the cover slip was then put onto a 100 µL of 0.5 % ice-cold glutaraldehyde/PBS solution and incubated for 15 min at 4 °C. Subsequently, the cover slips were transferred to a standard 12 well plate with the coated side up. Cover slips were gently washed three times with PBS at RT followed by an incubation with sodium borohydride (5 mg/mL in PBS) for 3 min at RT. Cover slips were again washed three times with PBS and subsequently resterilised in 70 % ethanol for 20 min at RT. From now on cover slips were handled in the tissue culture hood. After three more washing steps in PBS cover slips were quenched in serum free medium for 1 hour at 37 °C. The coating of cover slips results in a red fluorescent background.

### **3.6.3 Growing cells on gelatine coated cover slips**

To observe the degradation of the extracellular matrix B16 melanoma cells (B16 F1 wt, B16 F1 scr, B16 F1 L6M5, B16 F1 L6E3, B16 F10 wt, B16 F10 scr, B16 F10 L8M2, B16 F10 L8E4) were plated on the gelatine coated cover slips generated in 3.6.2. The degradation of the extracellular matrix results in black areas on the cover slips. Cells were grown on cover slips for 20 hours. After this time cells were fixed for 20 min with 3 % PFA.

### 3. Methods

---

#### **3.6.4 Phalloidin staining of the cells**

To visualise the actin cytoskeleton cells were stained with phalloidin labeled to Alexa 488. Phalloidin is a toxin of the death cap (*amanita phalloides*) which binds to F-actin.

For the phalloidin staining cells were incubated with a blocking and permeabilisation solution (3% BSA/0.1% Saponin/PBS) for 30 min at RT. Next the cells were incubated with the phalloidin antibody (1:1000) for 1 hour at RT followed by three washing steps in PBS for 10 min. Cells were embedded in Mowiol for confocal microscopy (3.6.5).

#### **3.6.5 Confocal microscopy of B16 melanoma cells grown on cover slips**

Images of the B16 melanoma cells that were grown on fluorescent gelatine cover slips were taken using an Olympus FV1000 confocal microscope and a 60× oil objective. Z-series of 200 cells per cell line were taken for analysis of the degradation of the extracellular matrix.

#### **3.6.6 Quantification of the degradation of the extracellular matrix**

For the quantification of the degradation of the extracellular matrix in B16 melanoma cell lines Image J was used. To this end, the number of cells was determined in the green channel of each picture. Then the red channel of each picture was turned into a black and white projection in which white shows the fluorescent background and black the degraded part of the background. The percentage of degraded area was ascertained by using particle analysis. The percentage of degraded area was divided by the number of cells of the according phalloidin stained picture to get the average degradation of a single cell. This procedure was done for 200 cells of each cell line.

### **3.7 Proliferation assay**

To determine the proliferation of B16 melanoma cell lines and to measure if there are differences in the proliferation rate between wildtype and knockdown cell lines  $2 \times 10^5$  cells of each cell line (B16 F1 wt, B16 F1 scr, B16 F1 L6M5, B16 F1 L6E3, B16 F10 wt, B16 F10 scr, B16 F10 L8M2, B16 F10 L8E4) were plated in standard 6 well plates. The number of cells was counted using the automated cell counter Countess™ (Invitrogen) according to the manufacturer's protocol after 24 hours, 48 hours and 72 hours. Each cell line was plated in triplicates for each time.

### 3. Methods

---

## 3.8 Western Blot

### 3.8.1 Cell lysates

To extract whole cell lysates, cells were washed twice in cold (4 °C) PBS. Cells then were pelleted at 1.200xg for 3 min at 4 °C and resuspended in 1 volume of CHAPS lysis buffer followed by incubation on ice for 30 min. Samples were centrifuged at 14.000xg for 20 min at 4 °C and supernatants (whole cell lysates) were recovered.

### 3.8.2 SDS polyacrylamid gelectrophoresis

Samples were heated in SDS sample buffer for 5 min at 100 °C and shortly centrifuged. Samples were then loaded on polyacrylamid gels (10 %) and run at 120 mV in SDS running buffer.

### 3.8.3 Blotting and detection

Proteins were blotted on nitrocellulose membranes (Protran, Schleicher & Schuell) for 90 min at 240 mA in blot transfer buffer. Afterwards membranes were blocked for 30 min in blocking buffer and incubated with primary antibody overnight at 4 °C. After washing membranes were incubated with secondary antibody for one hour at RT, followed by the detection of signals on film (Amersham Inc.) using enhanced chemiluminescence (ECL reagent, Pierce).

## 3.9 Migration assay B16 mouse melanoma cells

B16 mouse melanoma cells were seeded on 12-well plates O/N and imaged at 37 °C using an Olympus IX81 inverted microscope with CO<sub>2</sub> supply. For each cell line (B16 F1 scr, B16 F1 L6M5, B16 F1 L6E3, B16 F10 scr, B16 F10 L8M2, B16 F10 L8E4) Phase contrast pictures were taken every 15 min over 10 hours, and movies were generated from the pictures using the software excellence RT from Olympus. Migration paths of individual cells were tracked in the movies using excellence RT software from Olympus.

From the migration paths total path length was calculated using excellence RT software. For each cell line, 100 cells were tracked in two independent experiments.

## 3.10 Statistical analysis

Results were expressed as mean  $\pm$  SEM. Statistical analysis were standard two-tailed student t test for two data sets using Prism (GraphPad Inc.). P values below 0.05 (\*), <0.01 (\*\*), and <0.001 (\*\*\*) were deemed as significant and highly significant, respectively.

## 4. Results

### 4.1 FAN mediates navigational capacity of leukocytes responding to wounds and infection

#### 4.1.1 Identification of zebrafish FAN

FAN is involved in TNF mediated actin reorganisation (Haubert et al. 2007) and leukocyte recruitment (Montfort et al. 2009). To test the function of FAN for leukocyte motility *in vivo* the zebrafish (*Danio rerio*) was used in this work as a model organism. The zebrafish embryo/larvae turned out to be a powerful model system to observe leukocyte function *in vivo* (Cvejic et al. 2008; Feng et al. 2010; Zhang et al. 2008). From this end, the first aim was to identify a FAN homolog in zebrafish, and the genomic databases ensemble ([http://www.ensembl.org/Danio\\_rerio/index](http://www.ensembl.org/Danio_rerio/index)) and NCBI (<http://www.ncbi.nlm.nih.gov>) were searched for FAN homologues. Both databases revealed one sequence that was predicted to be a FAN homolog, but both of these fragments were too short to represent the whole zebrafish FAN. Sequence alignment of the two predicted zebrafish FAN homologues with mouse FAN cDNA revealed that the sequence found in ensemble has high homology to the N-terminal part of mouse FAN cDNA while the sequence found in NCBI shows high homology with the C-terminal part of mouse FAN cDNA. To test if both fragments represent only one homolog FAN specific PCR-Primer were designed and PCRs from cDNA generated from zebrafish embryos 2 days postfertilization (dpf) were performed. Here, the forward primers bound to the fragment predicted to be the N-terminal part of zebrafish FAN, the reverse primers bind to the part predicted C-terminal part of zebrafish so a product could only be observed if both parts represent one homolog (Fig.3). Indeed, both identified sequences represent only one zebrafish FAN homolog, and the PCR fragment corresponding to the full-length zebrafish FAN was sequenced for further analysis (Fig. 3A). The zebrafish FAN gene encodes a protein with 911 amino acids and shows the typical signature of three functional domains: a weakly conserved PH domain (amino acid 191 – 286), a BEACH domain (amino acid 302 - 575) and five WD40 domains at the C-terminus (amino acid 625 – 911) (Fig. 3B).

## 4. Results

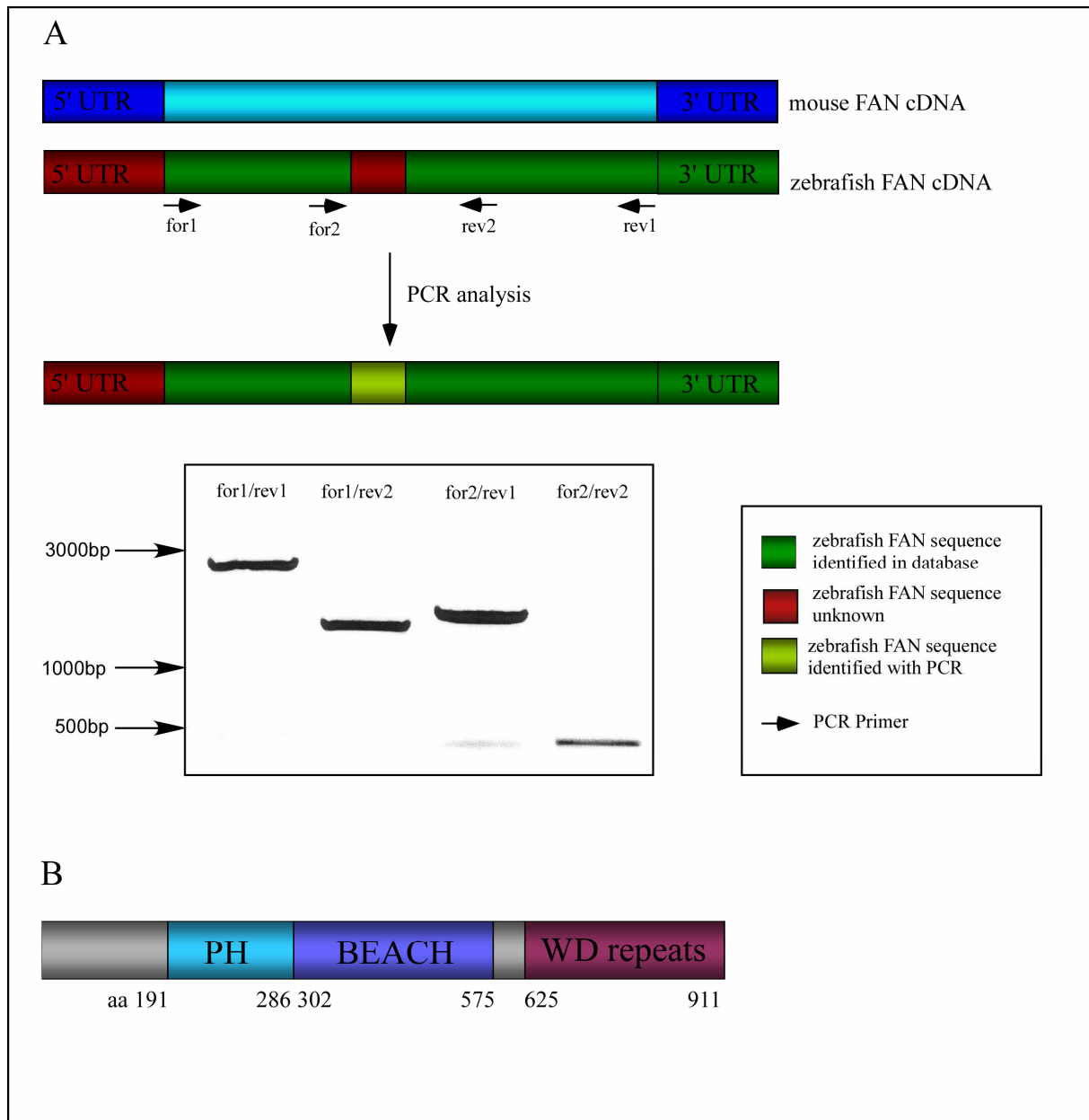


**Figure 3:** A) Schematic drawing of the cloning strategy used to amplify zebrafish FAN. The forward primers bind to the fragment predicted to be the N-terminal part of zebrafish FAN, the reverse primers bind to the predicted C-terminal part of zebrafish generating a product only if both parts represent one homolog. B) Schematic drawing of the primary structure of zebrafish FAN. The PH, BEACH and WD40 domains are shown in light blue, dark blue and purple, respectively.

Sequence alignments of FAN from different species were made using Vector NTI (Invitrogen). Sequence comparison between mouse and zebrafish FAN revealed a total homology of 70 % and a consensus homology of 78.5 % (Figure 4). This high degree of conservation of FAN is observed in the entire animal kingdom suggesting its evolutionary conserved role in cellular processes.

## 4. Results



**Figure 4:** Sequence comparison between zebrafish, mouse and human FAN. Sequence comparison between mouse and zebrafish FAN revealed a total homology of 70 % and a consensus homology of 78.5 %.

### 4.1.2 Morpholino knockdown in zebrafish embryos

To determine if FAN is expressed during the early stages of development, which is essential for morpholino (MO) knockdown, RT-PCR analysis was performed. mRNA was isolated from embryos at the indicated time points post-fertilization (pf), and  $\beta$ -Actin was used as a positive control. FAN mRNA is already maternally provided and strongly expressed during the first 6 days of development, which indicates a possible role of FAN during early developmental stages (Fig. 5A). After having verified the FAN expression during the early stages of development morpholinos were designed for FAN knockdown. Two so called splice Morpholinos were designed which bind to the boundaries of Intron1/Exon2 (I1E2) and Exon2/Intron2 (E2I2) masking the splicing sites of Exon2 (Fig 5B). Thus, splicing sites of Exon2 are masked and Exon2 is abolished in the mature mRNA which results in the generation of stop codons in Exon3 and therefore in a nonfunctional protein (Fig. 5B). To apply morpholino induced knock-down of FAN, one cell stage embryos were injected with FAN morpholinos and the efficiency of FAN knock-down was monitored by RT-PCR. Injection of the single Morpholinos (I1E2, E2I2) and double injection (DI) abolished the wt-transcript. The double injection of both Morpholinos lead to the generation of two shorter splice variants. Sequence analysis of the two generated transcripts revealed a deletion of exon 2 and 3 and parts of exon 4 within the shorter transcript. Single injections were performed with a morpholino concentration of 0.3 mmol. Double injections were performed with a morpholino concentration 0.3 mmol and 0.6 mmol (Fig. 5C). Both splice variants have a frameshift caused by the deletion of exons resulting in a truncated protein.

To test if the knockdown of FAN had any impact on total numbers of leukocytes in FAN morphants, *in situ* hybridisation was performed using a probe against L-plastin, a marker for early leukocytes in zebrafish. In situ hybridization revealed that FAN morphant and control embryos have equal numbers of l-plastin positive cells (Fig. 5D).

## 4. Results

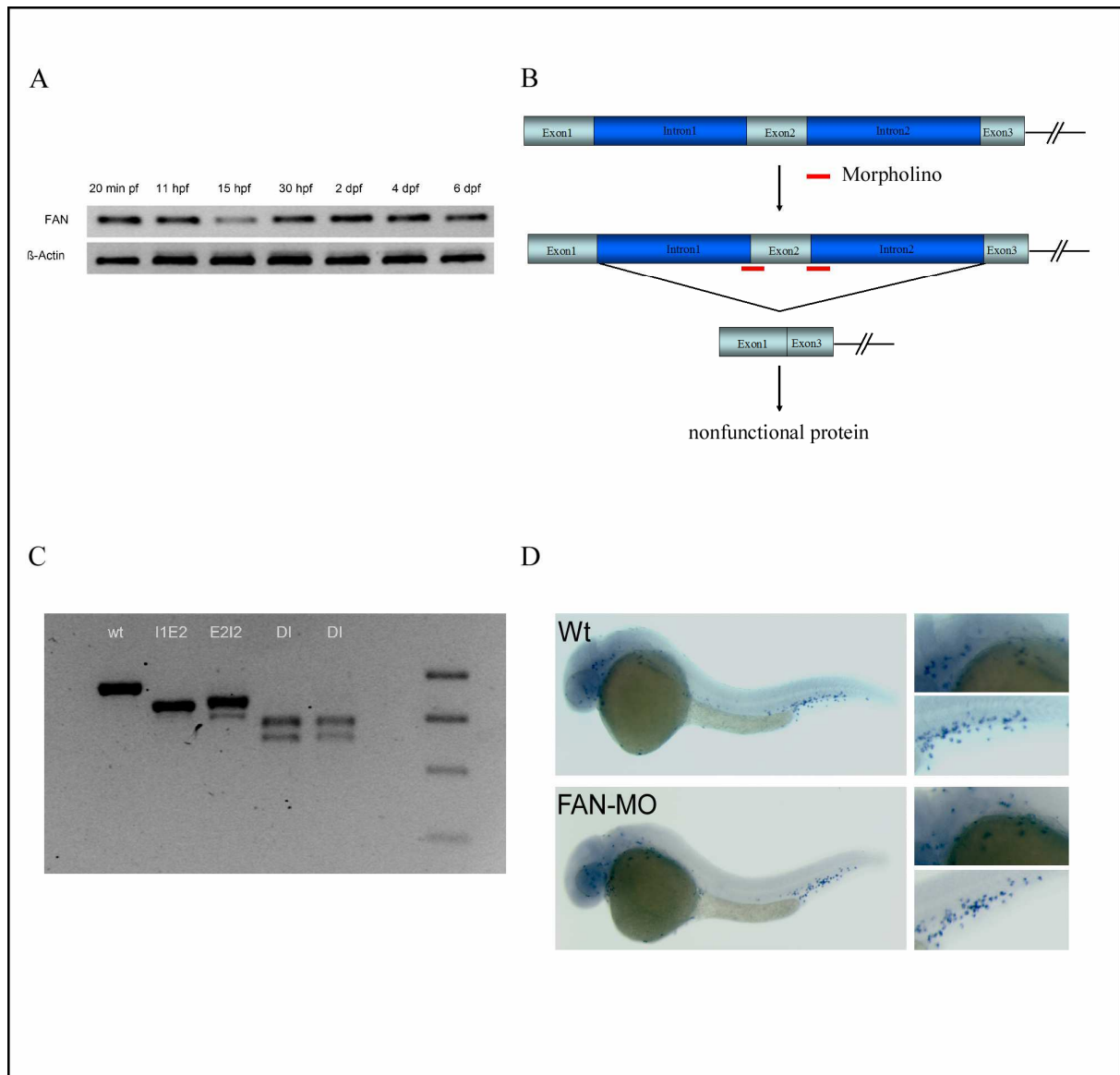


**Figure 5:** A) RT-PCR analysis of FAN during the early stages of development. mRNA was isolated from embryos at the indicated time points,  $\beta$ -Actin was used as a positive control. FAN mRNA is already maternally provided and strongly expressed during the first 6 days of development. B) Schematic drawing of the targeting strategy of FAN morpholino knockdown. Morpholinos that bind to the Intron1/Exon2 and Exon2/Intron2 boundary were designed to abolish Exon2 in the mature mRNA, resulting in a nonfunctional protein C) RT-PCR to monitor the effect of the injected FAN antisense Morpholinos. Injection of the single Morpholinos (I1E2, E2I2) and combined injection (DI) abolishes the wt-transcript. The combined injection of both Morpholinos leads to the generation of two shorter splice variants. Sequence analysis of the two generated transcripts revealed a deletion of exon 2 and 3 and parts of exon 4 within the shorter transcript. Single injections were performed with a morpholino concentration of 0.3 mmol. Double injections were performed with a morpholino concentration 0.3 mmol and 0.6 mmol. D) Whole mount in situ hybridization for l-plastin to visualize early leukocytes at 32 hpf. Small pictures on the right side are zoom-in areas for the head and the tail. No difference in number and distribution between wt and FAN knockdown embryos could be detected.

### 4.1.3 FAN propels leukocytes motility during wound response

To investigate the role of FAN in leukocyte motility either FAN specific MOs or a control MO was injected into one-cell stage embryos and their wound inflammatory response was compared at 2 dpf. For further experiments, unless otherwise indicated the PU1-Gal4-UAS-GFP zebrafish line was used, that expresses GFP in leukocytes allowing their observation *in vivo* (Peri et al. 2008). 2 dpf embryos were injured with a cutting laser at the end of the tail fin and the leukocytes that had reached the area indicated by the dashed line (Fig. 6A) were counted after 1.5 hours. The number of leukocytes that reached the wound 1.5 hours after injury was significantly reduced in FAN-MO injected embryos compared to control embryos. On average only  $1.9 \pm 0.32$  leukocytes reached the wound in FAN-MO injected embryos, whereas  $4.3 \pm 0.39$  and  $4.7 \pm 0.22$  leukocytes were counted in control and wild-type embryos, respectively (Fig. 6B).

To reveal if the reduced number of leukocytes at the site of injury affects both, the recruitment of macrophages and neutrophils, in a new set of experiments the total number of leukocytes labelled in the PU1-Gal4-UAS-GFP line was compared to the number of neutrophils responding to injury. To achieve this, neutrophils were visualized by sudan black staining in PU1-Gal4-UAS-GFP transgenic fish. Again, the total number of leukocytes recruited to the wounds was reduced in morphant embryos compared to control embryos. In control embryos on average  $4.5 \pm 0.34$  leukocytes reach the site of injury while in morphant embryos only  $3 \pm 0.35$  leukocytes reach the site of injury. The number of neutrophils in morphants was reduced to  $0.7 \pm 0.17$  compared to  $1.6 \pm 0.34$  in control embryos (Fig. 6 C, D, E). To determine the average number of macrophages the number of neutrophils was subtracted from the total number of leukocytes. This shows a recruitment of 2.9 macrophages in control embryos compared to 2.3 macrophages in morphant embryos. In summary the number of both, macrophages and neutrophils, is reduced in FAN-MO embryos. However there is a stronger reduction in neutrophil recruitment than in macrophage recruitment (Fig 6 E, F), which is in line with the observations made by Montfort et al.

In another set of experiments a double transgenic line (PU1-Gal4-UAS-RFP; MPX-GFP) was used to observe the number of leukocytes recruited to the wound. The total number of leukocytes is marked by PU1-Gal4-UAS-RFP (Sieger et al. in press), while neutrophils are marked with MPX-GFP (Renshaw et al. 2006). Also in this experiments the number of both, macrophages and neutrophils that were recruited to the wound was reduced in FAN morphant embryos (Fig. 6 F).

## 4. Results

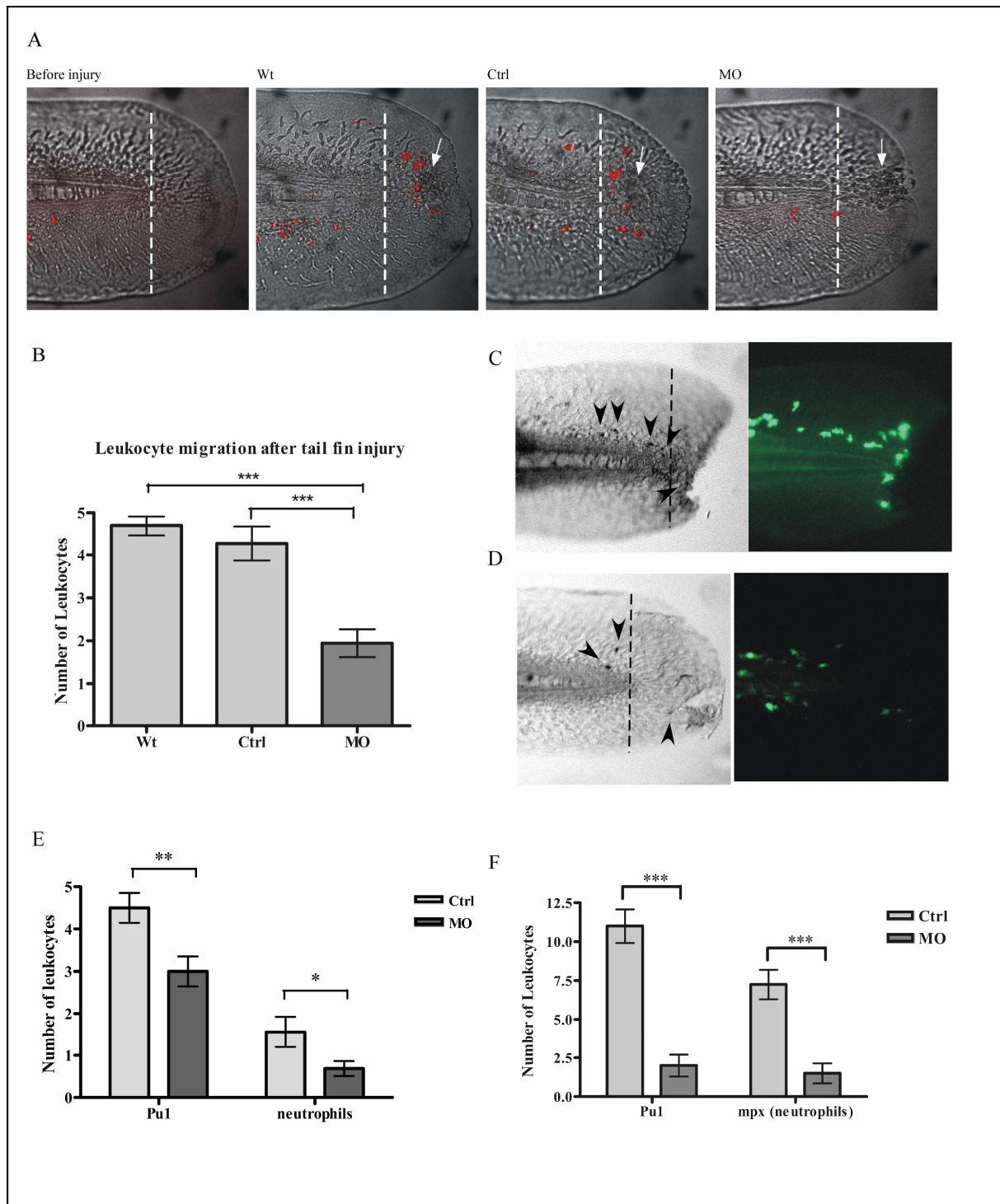


**Figure 6:** A) Tail fin of a zebrafish embryo before laser injury and wild-type, control and FAN-MO injected embryo 1.5hours after laser injury. The white arrow indicates the position of injury. The dashed line indicates the area in which leukocytes were counted after 1.5 hours. B) Statistical analysis of the number of leukocytes recruited to wt, control and morphant wounds. (wt n=19, ctrl n=20, MO n=35; p value wt/MO < 0.001\*\*\*, p value ctrl/MO < 0.001\*\*\*) C+D) Sudan Black Staining in Pu1-GAL4-UAS-GFP embryos. Embryos were injured with a scalpel and fixed 2h after tail fin injury. Green cells represent the total number of leukocytes that were recruited to the wound, neutrophils were stained with sudan black (arrowheads). The dashed line indicates the area in which leukocytes were counted after 1.5 hours. Results were expressed as mean  $\pm$  SEM. E) Statistical illustration of the total number of leukocytes and the number of neutrophils recruited to control and morphant wounds. (ctrl n=16, MO=15; p value ctrl/MO (Pu1) < 0,005\*\*, p value ctrl/MO (sudan black) < 0,03\*) F) Statistical illustration of the total number of leukocytes and the number of neutrophils recruited to

## 4. Results

control and morphant wounds in double transgenic embryos (PU1-Gal4-UAS-RFP; MPX-GFP) (Ctrl n=5, MO n=5) p value ctrl/MO (PU1) < 0.001\*\*\*, p value ctrl/MO (MPX) < 0.001\*\*\*)

### 4.1.4 FAN is required for the oriented migration of leukocytes

The observed migration defect that results in fewer leukocytes reaching the side of injury might be due to a slower movement of leukocytes. Alternatively, FAN knockdown might lead to a defect in the chemotactic migratory response and therefore results in less leukocytes at the site of injury. To further characterise the motility defect in FAN-MO injected embryos and to determine if this is secondary to a reduced velocity of leukocytes or to a defect in chemotactic migratory response, time-course series for 3 hours after injury were performed and the movement of leukocytes was tracked using Imaris software (Fig 7A). Speed analysis of the leukocytes showed that the overall speed of leukocytes in FAN-MO-injected embryos does not significantly differ from that in control and wild-type embryos (Fig. 7B). Thus, the lower number of leukocytes that reaches the wound after 1.5 hours (Fig. 6A, B) is not due to a reduction of velocity.

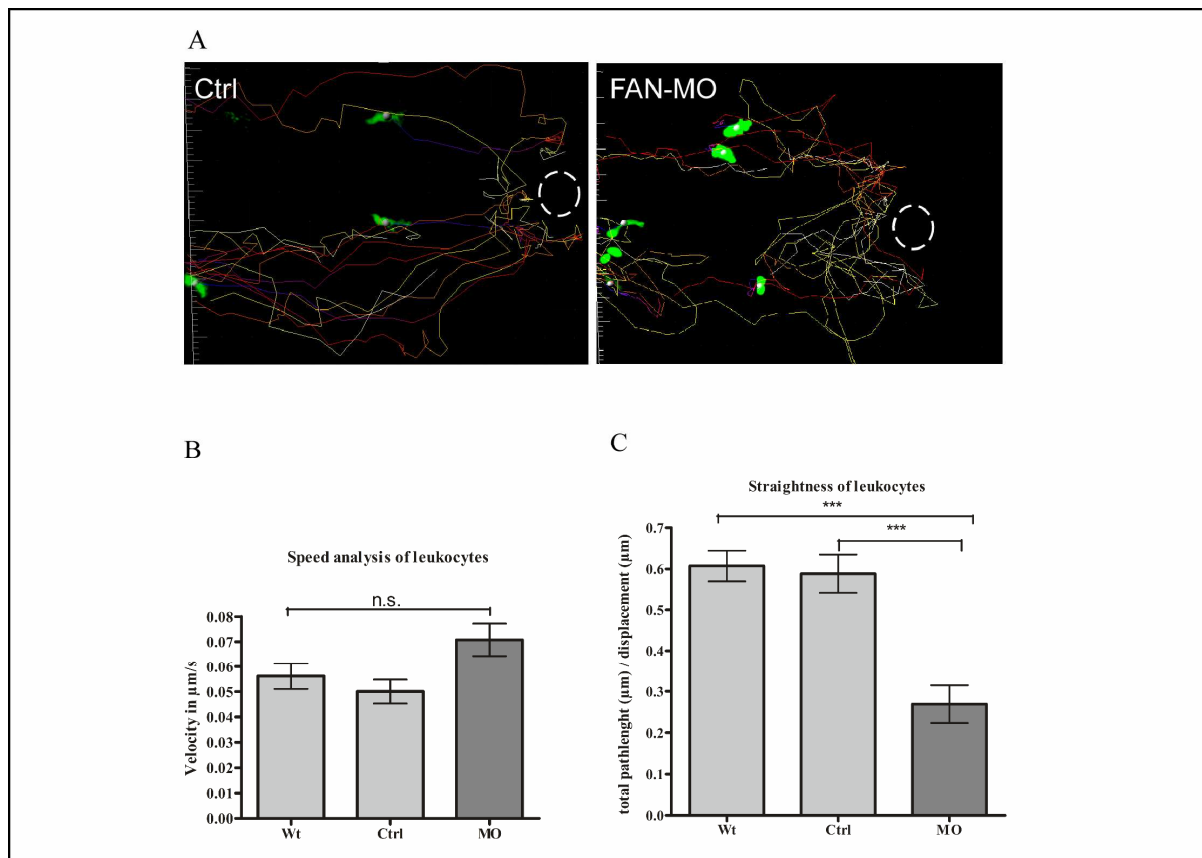


**Figure 7:** A) Cell tracking from fluorescence movies up to 3 hours after injury at the tail fin from 2dpf embryos treated with control or FAN morpholino. The dashed circle marks the site of injury B) Statistical illustration of the speed of leukocytes recruited to wounds in wt, control and morphant embryos. (wt n=18, ctrl n=18, MO n=26; p value wt/MO < 0.1 n.s) C) Statistical illustration of the

## 4. Results

---

straightness of leukocytes recruited to wounds in wt, control and morphant embryos. (wt n=18, ctrl n=18, MO n=26; p value wt/MO < 0.001\*\*\*, p value ctrl/MO < 0.001\*\*\*). Results were expressed as mean  $\pm$  SEM.

Since the speed of leukocytes in FAN knockdown embryos and siblings was comparable, the movement of leukocytes was analysed in greater detail. The number of leukocytes that move toward the wound in control embryos is larger than that in FAN-MO injected embryos. Tracking of the leukocytes revealed that in control embryos leukocytes move straight toward the wound and remain there after reaching it (Fig. 7A, and Fig. 8A, B). In contrast, in FAN-MO injected embryos, leukocytes do not start directly to move toward the wound, they extend protrusions in every direction before they start to move toward the wound. Furthermore, they do not move directly toward the site of injury, but rather move in another direction ending up in a circular movement, never reaching the wound (Fig. 7A and Fig. 8C, D). In addition, FAN-MO leukocytes that reach the wound often leave it again and some leukocytes stop on their way to the wound, turn around and disappear again, which was never observed in control embryos (Fig. 7A). To measure this movement of leukocytes towards the wound, the straightness, which is the quotient of the total path-length divided by the displacement (netto length) of a tracked leukocyte, was calculated. Investigation of the straightness revealed a significant difference between FAN-MO injected embryos wild-type and control embryos (Fig. 7C). In control and wild-type embryos the straightness of leukocyte movement is  $0.59 \pm 0.05$  and  $0.61 \pm 0.04$  whereas in FAN MO-injected embryos it is reduced to  $0.27 \pm 0.04$ . This reduction results in fewer number of leukocytes at the site of injury after 1.5 hours in FAN knockdown embryos (Fig. 6A).

Notably, the morphology of migrating leukocytes in FAN morphant embryos appears different to that of control embryos. In control embryos leukocytes have the typical shape with several pseudopodia at their leading edge and a retracting part without pseudopodia (Fig. 9A). In FAN morphant embryos leukocytes often do not have a clear leading edge and they extend pseudopodia in all directions (Fig. 9B). They retract these pseudopodia and then extend new pseudopodia in other directions without moving (Fig. 10). In addition, leukocytes in FAN knockdown embryos have more pseudopodia compared to control embryos (74 per leukocyte versus 33 in control embryos) and these cells more frequently made the “wrong” choice of pseudopodia (49.2%, versus 33.9% wrong turns in control embryos) (Fig. 9C).

## 4. Results

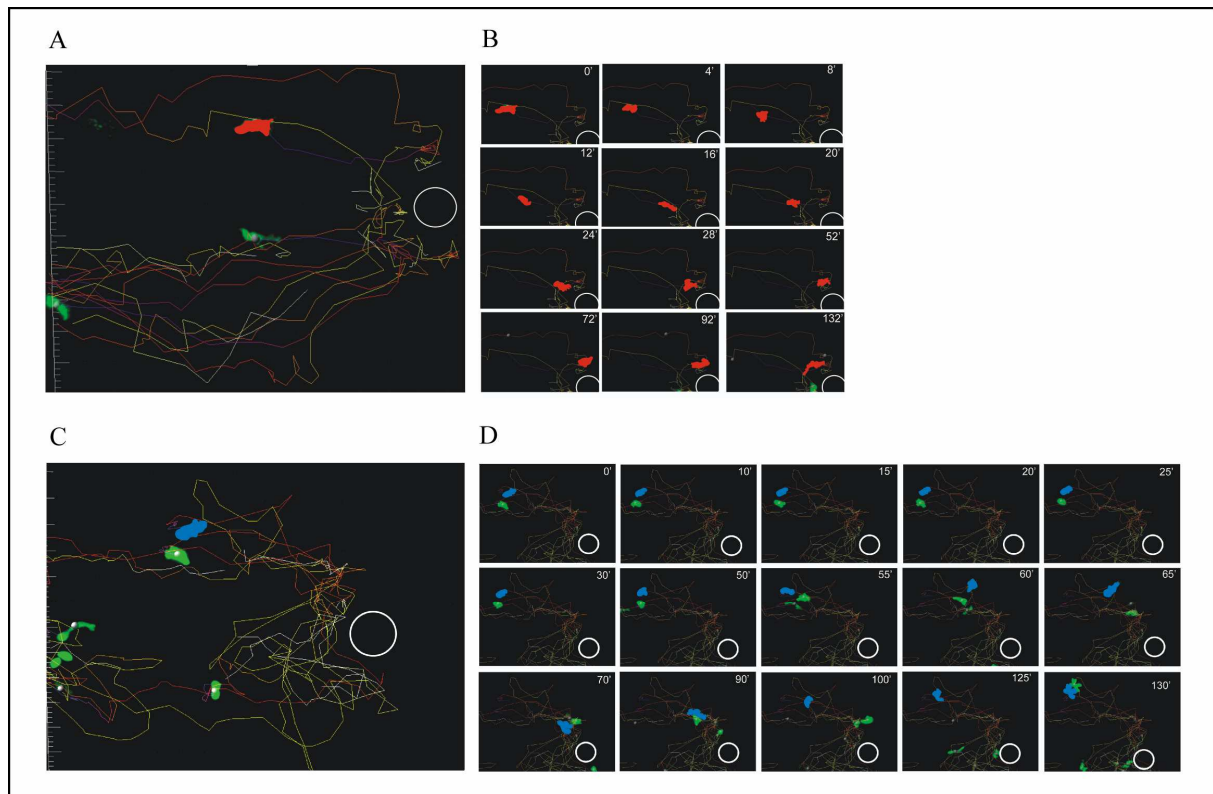


**Figure 8:** A) Overview of cell tracking of a wt embryo. The white circle indicates the site of injury. B) Detailed cell tracking of one leukocyte (red). The leukocyte moves directly toward the wound and reaches it after 24'. After reaching the wound it stays there and does not move away from it. C) Overview of cell tracking of a FAN morphant embryo. The white circle indicates the site of injury. D) Detailed cell tracking of one leukocyte (blue). The leukocyte does not move directly toward the wound but performs protrusions in every direction before starting to move after 55'. After 70' the leukocyte reaches the wound but directly starts to move away again.

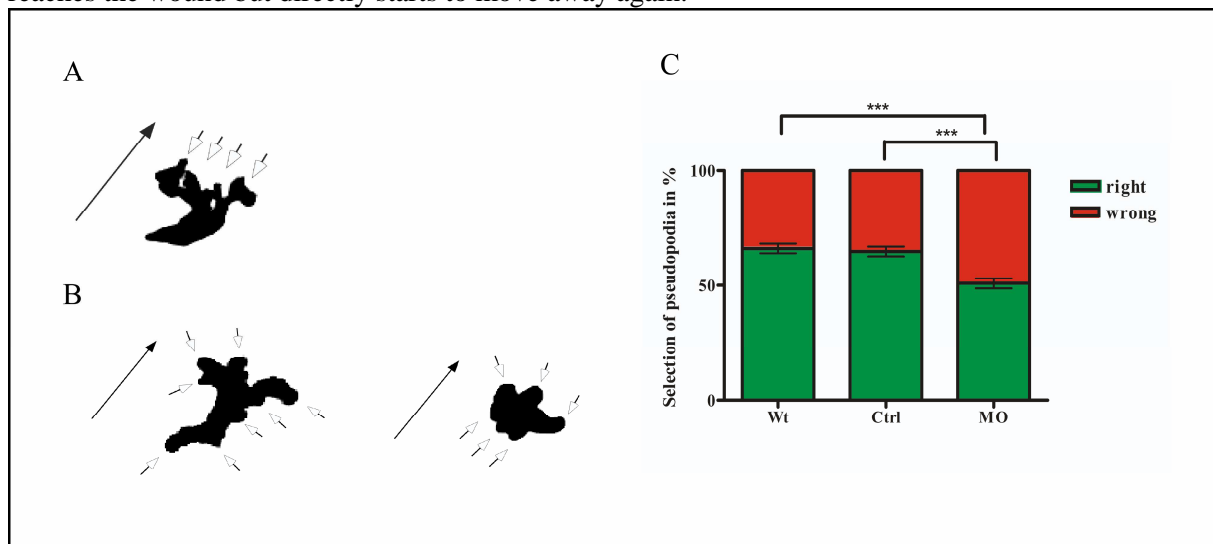


**Figure 9:** A) A typical shape of a control leukocyte. Leukocytes have one clear leading edge and a retracting part without pseudopodia. The black arrow indicates the direction of move. White Arrows indicate pseudopodia. B) A typical shape of morphant leukocytes. Leukocytes extend pseudopodia in all directions without having a clear leading edge. Arrow indicates the direction of move. White arrows indicate pseudopodia. C) Graphic illustration of the proportion of “right” choices (green) versus “wrong” choices (red) of pseudopodia made by control and wild-type versus morphant leukocytes. (Number of leukocytes: wt n=10, ctrl = 10, MO= 10; p value wt/MO<0.001\*\*\*, p value ctrl/MO < 0.001\*\*\* ). Results were expressed as mean  $\pm$  SEM.

#### 4. Results

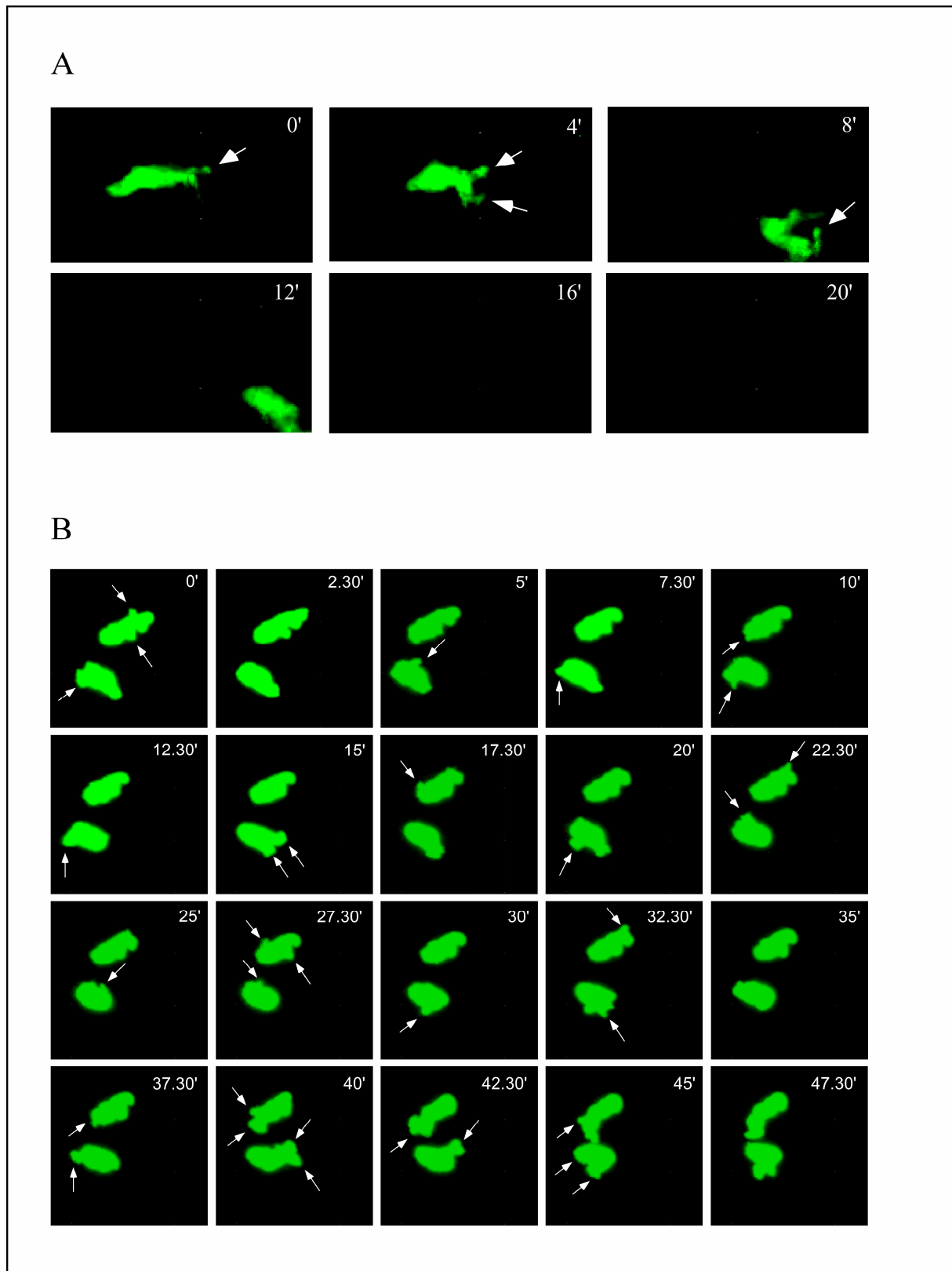


**Figure 10:** A) Time series of a wild-type leukocyte. The leukocyte starts moving directly toward the wound and extends protrusion only in the direction of motility. B) Time series of morphant leukocytes. The leukocytes extend protrusions in all direction and retract them again without moving. Even 47.30 minutes after injury the leukocytes have not started to move toward the tail fin wound

## 4. Results

---

Taken together, the role of FAN in leukocyte motility was described here for the first time *in vivo*. Leukocytes of FAN knockdown embryos do not move slower than their siblings in wildtype embryos but have a reduced straightness, exhibit an abnormal shape with more pseudopodia in the wrong direction and thus reach the site of injury less efficiently. These findings are in line with previous observations in cultured FAN-deficient MEFs showing altered cell polarity in a wound-scratch test upon TNF treatment (Haubert et al. 2007).

### 4.1.5 FAN propels leukocytes motility during infection response

To test if the difference in leukocyte migration is tissue or stimulus dependent, the otic placode of 2 dpf embryos was infected with red fluorescent *E.coli* and the numbers of leukocytes reaching the site of infection was counted 30 min post infection (Fig. 11). Statistical analysis demonstrated that in this infection model, the number of leukocytes that reach the site of infection is significantly reduced in FAN morphant leukocytes (Fig. 11 B, C). In control and wild-type embryos on average  $15.25 \pm 1.8$  and  $15 \pm 0.94$  leukocytes reach the site of infection whereas only  $9 \pm 0.85$  leukocytes appear in FAN morphant embryos. This experiment provides evidence that the migration defect of leukocytes in morphant embryos is not tissue or stimulus dependent and implies a general role for FAN in the chemotactic migratory response.

In addition leukocytes in FAN morphant embryos seem to show a decreased phagocytosis rate. (Fig. 11 D, E). To reveal if there is less bacterial uptake in morphant embryos colocalisation analysis was performed. Colocalisation analysis revealed a colocalisation rate for macrophages and bacteria of  $0.13 \pm 0.04$  in FAN morphant embryos compared to  $0.51 \pm 0.17$  in control embryos.

## 4. Results

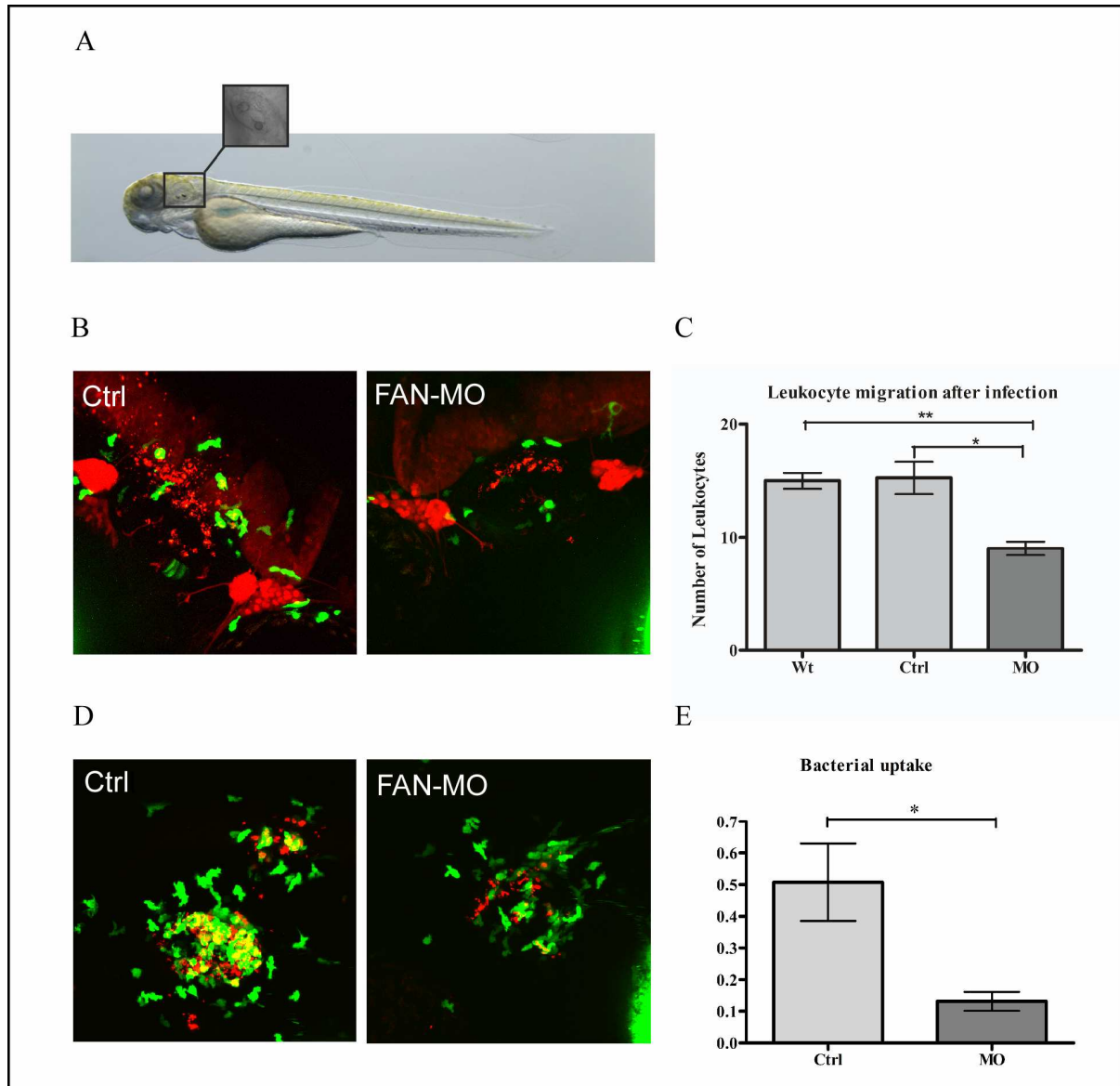


**Figure 11:** A) 3dpf zebrafish larvae. The black rectangle marks the optic tectum, which is shown in a higher magnification on top. B) Fluorescent images of the optic tectum infected with dsRED labeled *E.coli* in control and FAN morphant embryos 30 minutes after infection. C) Statistical illustration of the number of leukocytes recruited to wt, control and morphant otic placodes after infection with red fluorescent *E.coli*. (wt n=5, ctrl n=5, MO n=6; p value wt/MO < 0.003\*\*, p value ctrl/MO < 0.01\*). Results were expressed as mean ± SEM.

D) Fluorescent images of the optic tectum infected with dsRED labeled *E.coli* in control and FAN morphant embryos 1.5 hours after infection. E) Statistical illustration of colocalisation analysis of leukocytes in control and morphant otic placodes after infection with red fluorescent *E.coli*. (Ctrl n=5, MO n=5; p value ctrl/MO < 0.04\*). Results were expressed as mean ± SEM.

### **4.2 FAN has an impact on cell migration, proliferation and matrix degradation in melanoma cells *in vitro***

#### **4.2.1 FAN knockdown in B16 mouse melanoma cells**

FAN is involved in TNF mediated actin reorganisation (Haubert et al. 2007) and leukocyte recruitment (Montfort et al. 2009). FAN deficient MEF cells exhibit a reduced migration after TNF stimulation (unpublished data, Dirk Haubert). In addition it was revealed in this work that FAN mediates navigational capacity of leukocytes responding to wounds and infection in zebrafish embryos *in vivo*. These findings implicate a general role for FAN in cell migration. Another cellular process that requires the migration of cells is metastasis. The motility of cancer cells, like normal cell motility, is driven by the reorganisation of the actin cytoskeleton and of contacts between the cell and the matrix, involving many of the same proteins required for normal cell motility. To test whether FAN is also involved in the migration of tumour cells and thus probably also in cancer cell metastasis two different B16 mouse melanoma cell lines were used. The B16 F10 mouse melanoma cell line, which was gained from the tenth generation of mouse melanoma cells (B16 F0 mouse melanoma cells) is a highly aggressive mouse melanoma cell line that develops many metastasis. The B16 F1 mouse melanoma cell line was gained from the first generation of mouse melanoma cells and is therefore a less aggressive mouse melanoma cell line.

To determine if FAN also has an impact on cancer cell migration and therefore probably also on metastasis of cancer cells, stable FAN knock-down melanoma cell lines were generated. For the knock-down of FAN the lentiviral system was used. First oligonucleotides for two different shRNAs were synthesised as described above (3.3). After annealing the oligonucleotides were cloned in the vector pENTR/siH1/mDD-Stuffer. To test if the shRNAs are functional, two pENTR/siH1/mDD-Stuffer, each bearing one of the two shRNAs were transiently co-transfected with pEGFP-C3/FAN into HEK293 FT cells. Co-transfection of pEGFP-C3/FAN was necessary because no functional antibody to detect FAN exists. As a control, pEGFP-C3 and untransfected HEK293FT cells were used. Western blot analysis revealed that FAN-EGFP is effectively down-regulated after co-transfection with the shRNA constructs while EGFP alone is not affected (Fig. 12A). After having proved that the shRNAs are functional, stable melanoma cell lines were generated. The FAN shRNA was recombined into the pLenti6/V5DEST-GFP by using directed attL/attR recombination and, virus was produced. Thereafter B16 F1 and B16 F10 melanoma cells were transduced with the virus and

## 4. Results

clones stably expressing the FAN shRNA stably integrated in their genome were selected by fluorescence and blasticidin resistance. To test which clones stably down-regulate FAN, quantitative real-time PCR analysis was performed. Two clones that stably down-regulate FAN in three independent experiments, each done in triplicate, were chosen for further experiments. For B16 F1 mouse melanoma cells, two clones, L6M5 and L6E3, were selected which express reduced levels of FAN of about 60% and 40% compared to wild-type FAN expression (Fig. 12B). For B16 F10 mouse melanoma cells, two clones, L8M2 and L8E4, were selected which express reduced levels of FAN of about 50% and 30% compared to wild type FAN expression (Fig. 12C).

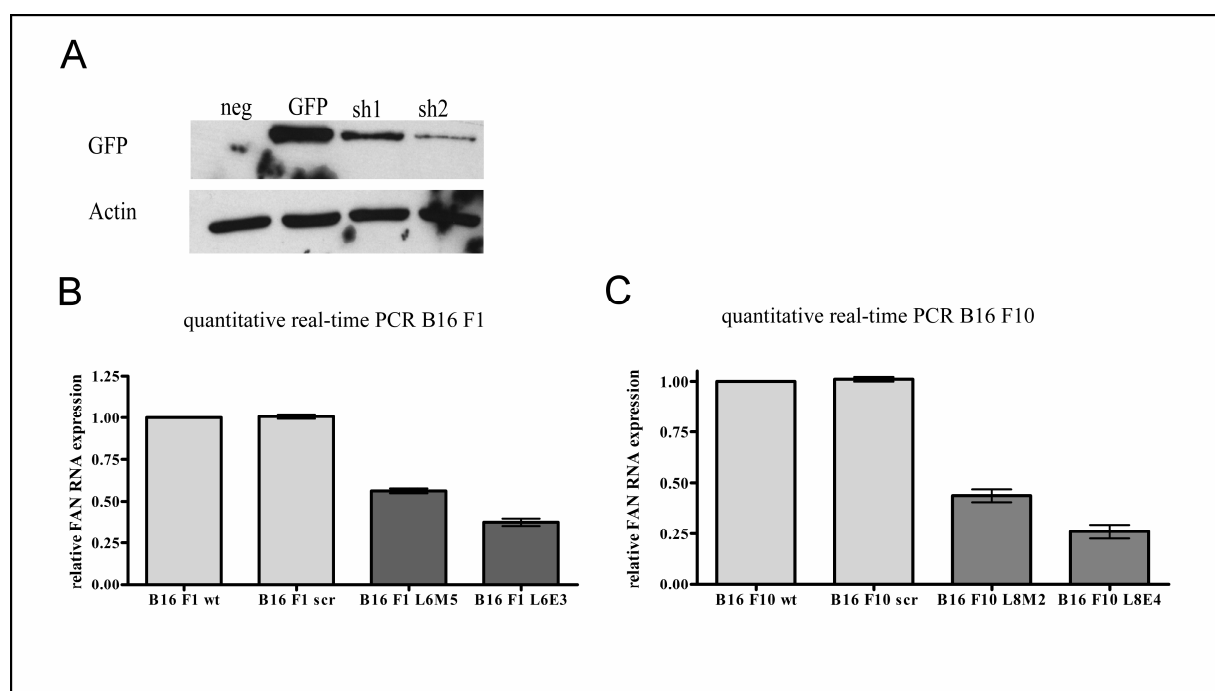


**Figure 12:** A) Western Blot analysis to test the functionality of FAN shRNA constructs. HEK 293 FT cells were either untransfected, transiently transfected with pEGFP-C3 alone or co-transfected with pEGFP-C3/FAN and one of the two pENTR/siH1/FANshRNA constructs. The GFP blot shows a down-regulation of the pEGFP-FAN when co-transfected with one of the shRNA constructs. B) Quantitative real time PCR to measure the relative FAN expression in B16 F1 FAN knockdown mouse melanoma cell lines. Two clones that stably down-regulate FAN in three independent experiments, each done in triplicate, were chosen for further experiments. C) Quantitative real time PCR to measure the relative FAN expression in B16 F10 FAN knockdown mouse melanoma cell lines. Two clones that stably down-regulate FAN in three independent experiments, each done in triplicate, were chosen for further experiments. Results were expressed as mean  $\pm$  SEM.

### 4.2.2 FAN knock-down in B16 mouse melanoma cell lines results in impaired migration induction after TNF stimulation

To reveal whether FAN knockdown also has an impact on cell migration in B16 mouse melanoma cells *in vitro* like it has in FAN morphant leukocytes in zebrafish embryos *in vivo*, cell migration assays were performed and the distance that was covered by each cell line was determined without and after TNF stimulation. Without TNF stimulation there is no difference in the path length between the different cell lines.

On average, B16 F1 scrambled, L6M5 and L6E3 cells migrate  $12.47 \pm 0.39$  mm,  $12.69 \pm 0.45$  mm and  $14.9 \pm 0.38$  mm in 10 hours, respectively. Migration of B16 F1 scrambled cells could be induced after TNF stimulation. B16 F1 scrambled cells migrated  $18.68 \pm 0.68$  mm compared to  $12.47 \pm 0.39$  mm without TNF stimulation. In contrast to this migration of the FAN knock-down cells was not inducible by TNF stimulation. L6M5 cells migrated  $14.4 \pm 0.41$  mm after TNF stimulation compared to  $12.47 \pm 0.39$  mm without TNF stimulation (Fig 13 A). The slight increase in migration can be explained by the fact that FAN expression is only reduced to 60 % in this cell line which might be enough for a minimal induction after TNF stimulation. L6E3 cell migration was not inducible by TNF stimulation, these cells migrated  $14.66 \pm 0.38$  mm compared to  $14.9 \pm 0.38$  mm without TNF stimulation.

The same results could be observed for the B16 F10 mouse melanoma cell lines. Again, there was no difference in the migrational behaviour of the three cell lines without TNF stimulation. The average distance of B16 F10 scrambled, L8M2 and L8E4 was  $11.60 \pm 0.38$  mm,  $11.56 \pm 0.37$  mm and  $12.31 \pm 0.36$  mm, respectively. After TNF stimulation for 10 hours, the average migration length of B16 F10 scrambled cells was increased to  $17.99 \pm 0.38$  mm. Cell migration in the B16 F10 mouse melanoma knock-down cell lines was not inducible with TNF. L8M2 cells displayed an average path length of  $12.73 \pm 0.37$  mm compared to  $11.56 \pm 0.37$  mm without TNF stimulation and L8E4 cells displayed an average path length of  $13.62 \pm 0.31$  mm compared to  $12.31 \pm 0.36$  mm without TNF stimulation (Fig. 13 B). These findings are in line with the observations found in migration assays performed in MEF cells (Dirk Haubert, unpublished data).

## 4. Results

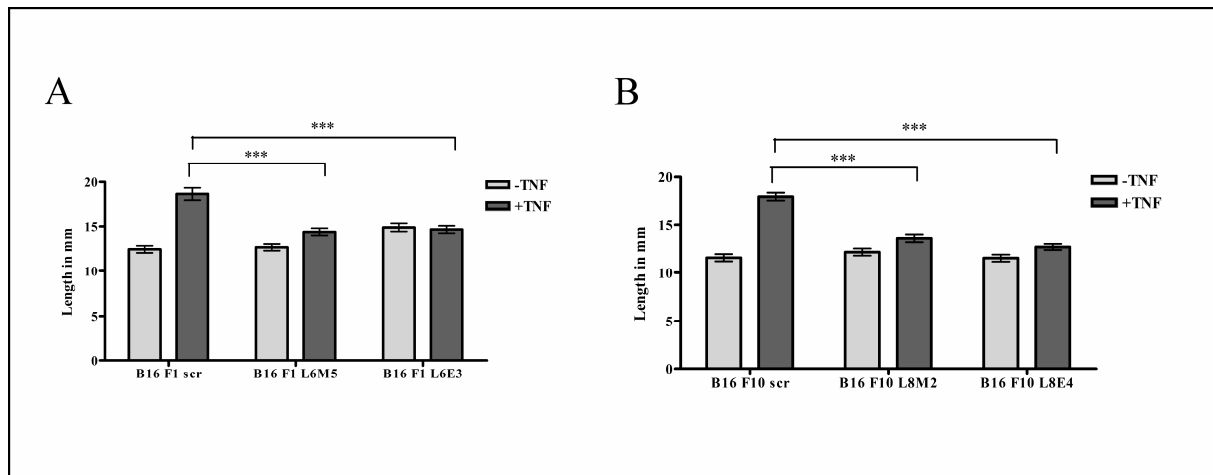


**Figure 13:** A) Migration in B16 F1 cell lines after TNF stimulation. Migration was measured every 15 min for 10 hours at 37 °C. B16 F1 scrambled cells show an induction of migration after TNF stimulation. B16 F1 scrambled cells migrate  $18.68 \pm 0.68$  mm compared to  $12.47 \pm 0.39$  mm without TNF stimulation. B16 F1 knock-down cells (L6M5 and L6E3) show no induction of migration after TNF stimulation. L6M5 cells migrate  $14.40 \pm 0.41$  mm compared to  $12.69 \pm 0.45$  mm without TNF stimulation and L6E3 cells migrate  $14.66 \pm 0.38$  mm compared to  $14.90 \pm 0.38$  mm without TNF stimulation. B) Migration in B16 F10 cell lines without and after TNF stimulation. Migration was measured every 15 min for 10 hours at 37 °C. B16 F10 scrambled cells show an induction of migration after TNF stimulation. B16 F10 scrambled cells migrate  $17.99 \pm 0.38$  mm compared to  $11.60 \pm 0.38$  mm without TNF stimulation. B16 F10 knock-down cells (L8M2 and L8E4) show no induction of migration after TNF stimulation. L8M2 cells migrate  $12.73 \pm 0.37$  mm compared to  $11.56 \pm 0.37$  mm without TNF stimulation and L8E4 cells migrate  $13.62 \pm 0.31$  mm compared to  $12.31 \pm 0.36$  mm without TNF stimulation. For the quantification 100 cells per cell line were analysed. Results were expressed as mean  $\pm$  SEM.

### 4.2.3 The degradation of the extracellular matrix is reduced in FAN knock-down mouse melanoma cells

B16 melanoma FAN knock-down cell lines exhibit an impaired induction of migration after TNF stimulation. For metastasis, cell migration is a necessity and cancer cells lacking FAN could be impaired in their ability to metastasis by the fact that cell migration is impaired in these cells. Another necessary condition for metastasis is the ability of cancer cells to degrade the extracellular matrix. If cancer cells are not able to degrade the extracellular matrix they are not able to get into the blood stream and settle down in distinct environments to develop metastasis. To test whether B16 mouse melanoma cells are impaired in matrix degradation after FAN knock-down, degradation assays were performed. Cells were plated on cover slips coated with red fluorescent gelatine, resulting in a red fluorescent background and areas with matrix degradation are recognised as black dots or black areas.

B16 F1 wild-type cells plated on a red fluorescent background exhibited black areas in the background after 20 hours (Fig. 14 A), indicating the degradation of the extracellular matrix.

#### 4. Results

---

B16 F1 scrambled cells also displayed these black areas (Fig. 14 B). L6M5 FAN knock-down cells displayed much less matrix degradation compared to wild-type and scrambled cells (Fig 14 C) and the same is true for the L6E3 cells (Fig. 14 D). To quantify the extent of matrix degradation in the different cell lines the percentage of black areas was determined for each cell line by using Image J software. Quantification revealed an extent of matrix degradation in B16 F1 wt and B16 F1 scrambled cells of 1.4 %. In L6M5 cells only 0.9% of the extracellular matrix was degraded and in L6E3 cells, the extent of degraded area was reduced to 0.3% (Fig. 16 A). For B16 F10 cell lines plated on red fluorescent background similar results could be observed. B16 F10 knock-down cell lines displayed less matrix degradation than B16 F10 wild-type and B16 F10 scrambled cells (Fig. 15). In B16 F10 wild-type and B16 F10 scrambled cells 2.0 % and 1.8 % of the extracellular matrix was degraded while in L8M2 cells the percentage of degradation was reduced to 0.5 % and in L8E4 cells only 0.3 % of the extracellular matrix was degraded (Fig. 16 B). The differences in the extent of matrix degradation between the two knock-down cell lines is due to the fact that in L6M5 and L8M2 cells FAN expression is only reduced to 60 % and 50 % of wild-type amount, respectively, while in L6E3 and L8E4 cells FAN expression is reduced to 40 % and 30 %, respectively.

In summary, B16 mouse melanoma cell lines showed a reduced induction of migration after TNF stimulation and they also degraded less extracellular matrix compared to their wild-type and scrambled counterparts.

Because FAN knock-down B16 mouse melanoma cells displayed a reduced migrational behaviour and reduced matrix degradation the next step was to examine the behaviour of B16 mouse melanoma cell lines *in vivo*.

4. Results

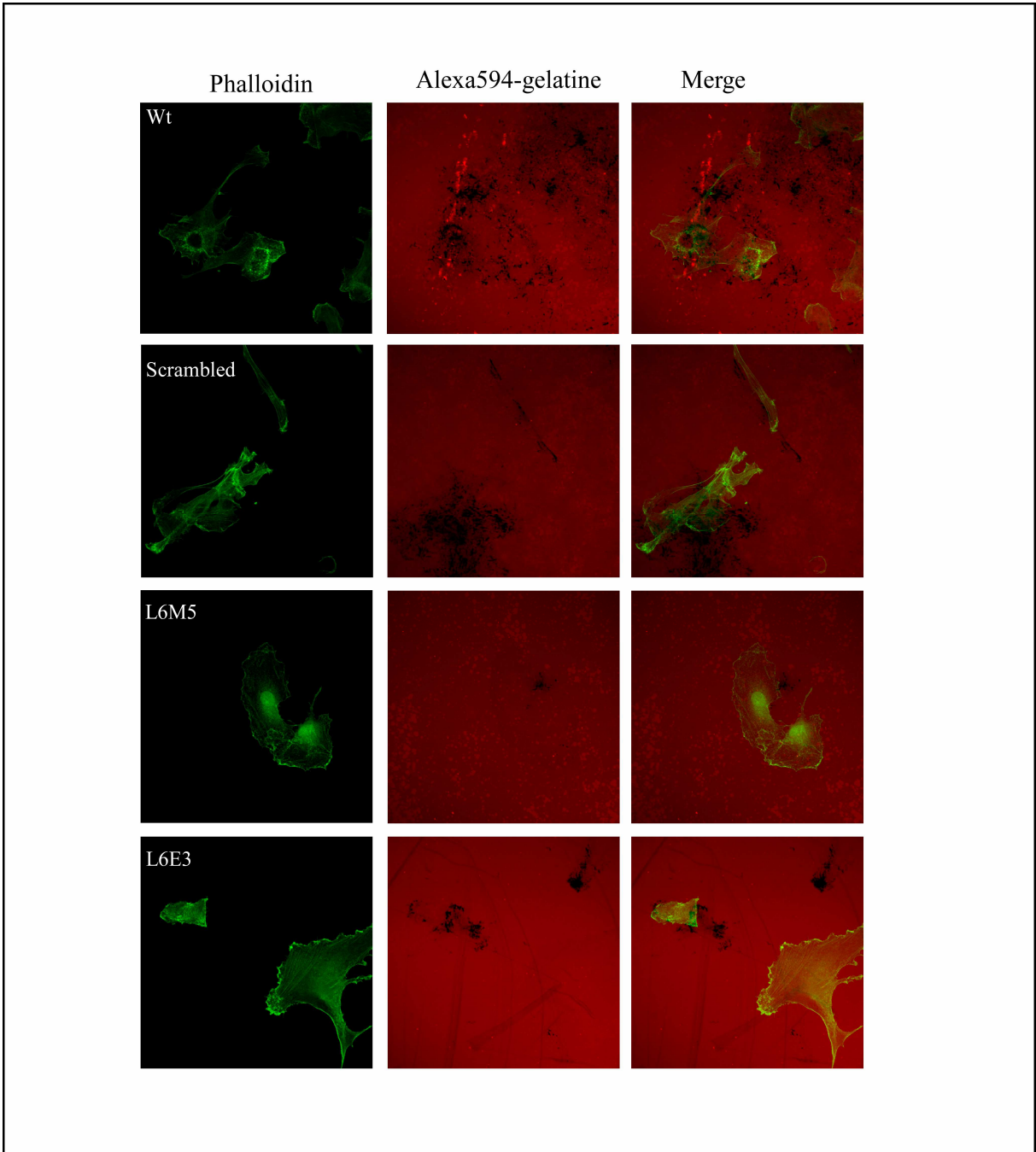


**Figure 14:** Degradation assay of B16 F1 mouse melanoma cells. Degraded matrix is visible as black areas in the red fluorescent background. green = Phalloidin, red = Alexa594-gelatine

4. Results

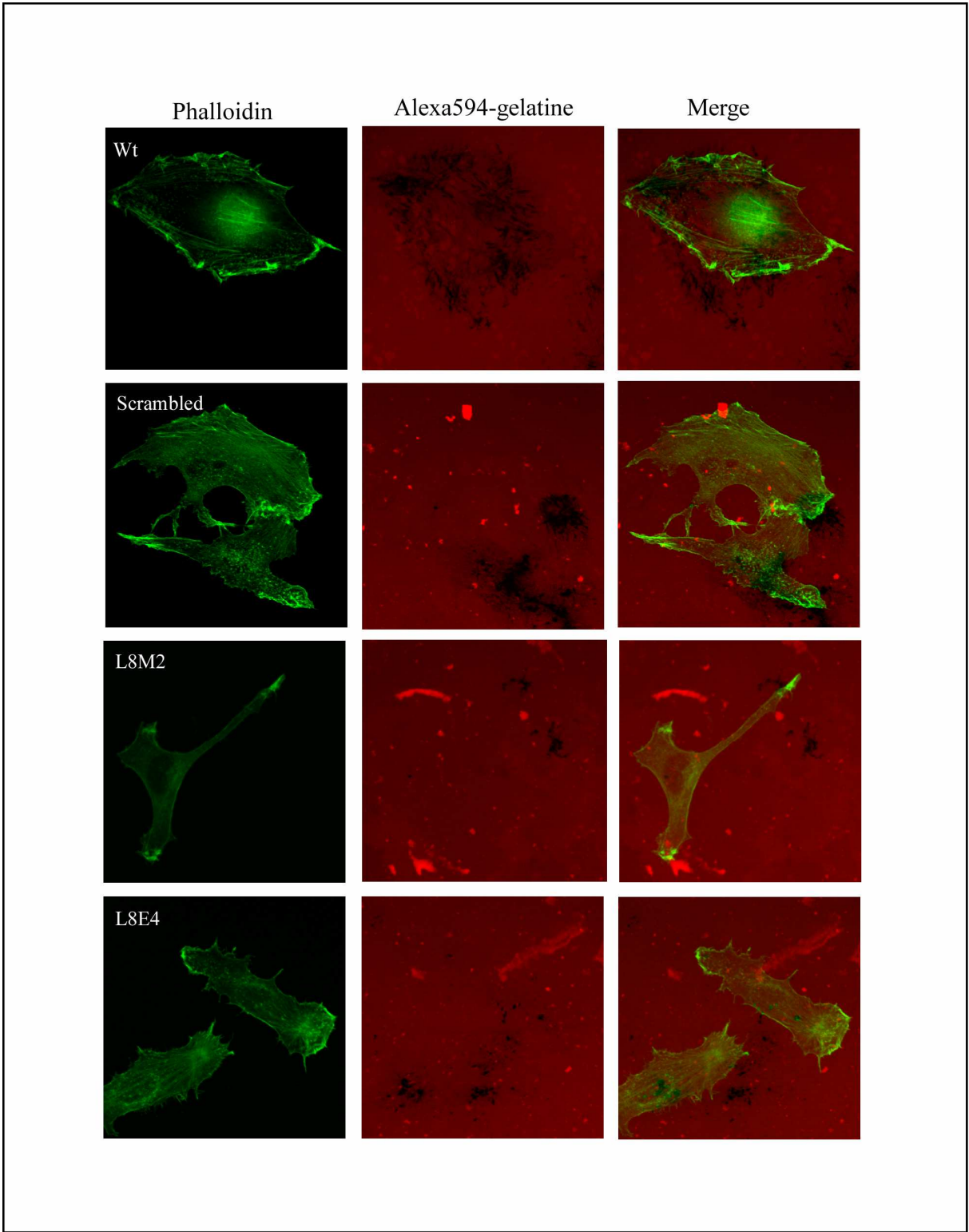


**Figure 15:** Degradation assay of B16 F10 mouse melanoma cells. Degraded matrix is visible as black areas in the red fluorescent background. green = Phalloidin, red = Alexa594-gelatine

## 4. Results

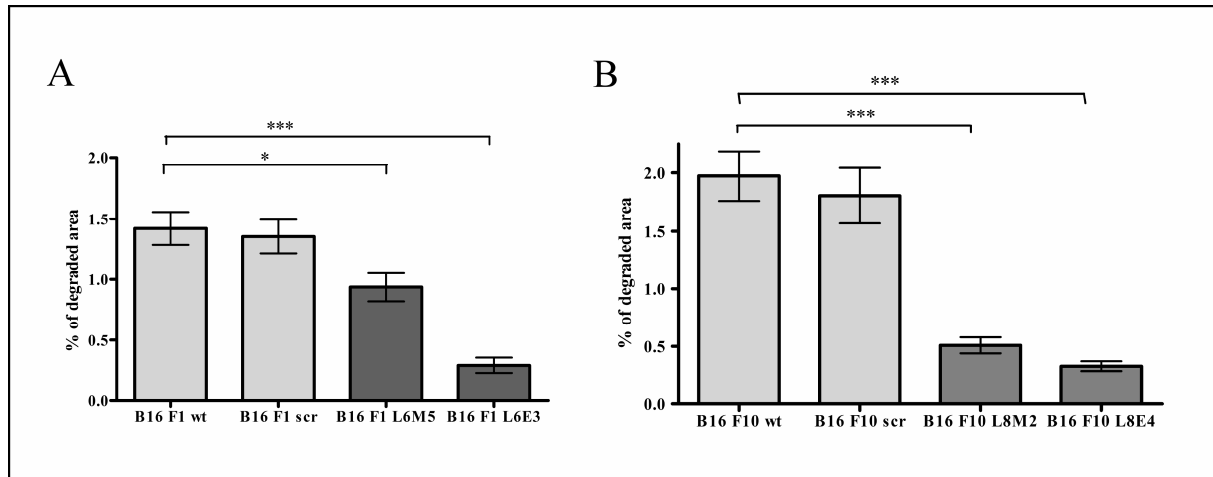


**Figure 16:** A) Quantification of the matrix degradation in B16 F1 mouse melanoma cell lines. In B16 F1 wt and B16 F1 scrambled cells 1.4 % of the extracellular matrix is degraded while in L6M5 and L6E3 cells the percentage of degradation is reduced to 0.9% and 0.3 %, respectively B) Quantification of the matrix degradation in B16 F10 mouse melanoma cell lines. In B16 F10 wild-type and B16 F10 scrambled cells 2.0 % and 1.8 % of the extracellular matrix is degraded while in L8M2 and L8E4 cells the percentage of degradation is reduced to 0.5 % and 0.3 %, respectively. (n=200 per cell line; p value F1 wt/F1 L6M5=0.01; p value F1wt/F1 L6E3 < 0.001; p value F10 wt/F10 L8M2 < 0.001; F10 wt/F10 L8E4 p < 0.001) Results were expressed as mean  $\pm$  SEM.

### 4.2.4 Mice injected with B16 mouse melanoma FAN knock-down cells display reduced tumour growth and metastasis

FAN knock-down B16 mouse melanoma cells display a reduced migrational behaviour and reduced matrix degradation *in vitro*. To test the metastatic behaviour of these cells *in vivo* mice were chosen as a model organism. For this purpose, B16 mouse melanoma cells were implanted subcutaneously into wild-type mice (C57BL/6) and the survival rate of these mice was determined. Mice implanted with B16 F1 wt cells all died within 24 days after implantation while 50 % of the mice that have been implanted with the B16 F1 knock-down cells (L6E3) were still alive at day 24. Mice implanted with B16 F10 wt cells all died within 27 days after implantation. At this time point 40 % of the mice that have been implanted with the B16 F10 knock-down cells (L8E4) were still alive. Taken together, mice that had implanted the B16 mouse melanoma FAN knock-down cell lines exhibited a higher survival rate (Fig. 17). In the next step, the tumour growth was observed by measuring the tumour diameter until day 24 after cell implantation. For both, B16 F1 and B16 F10 cell lines, the tumours in mice implanted with the knock-down cell lines were detectable later than the tumours of the corresponding wild-type cell lines and they display smaller diameters (unpublished data, Nikola Baschuk).

## 4. Results

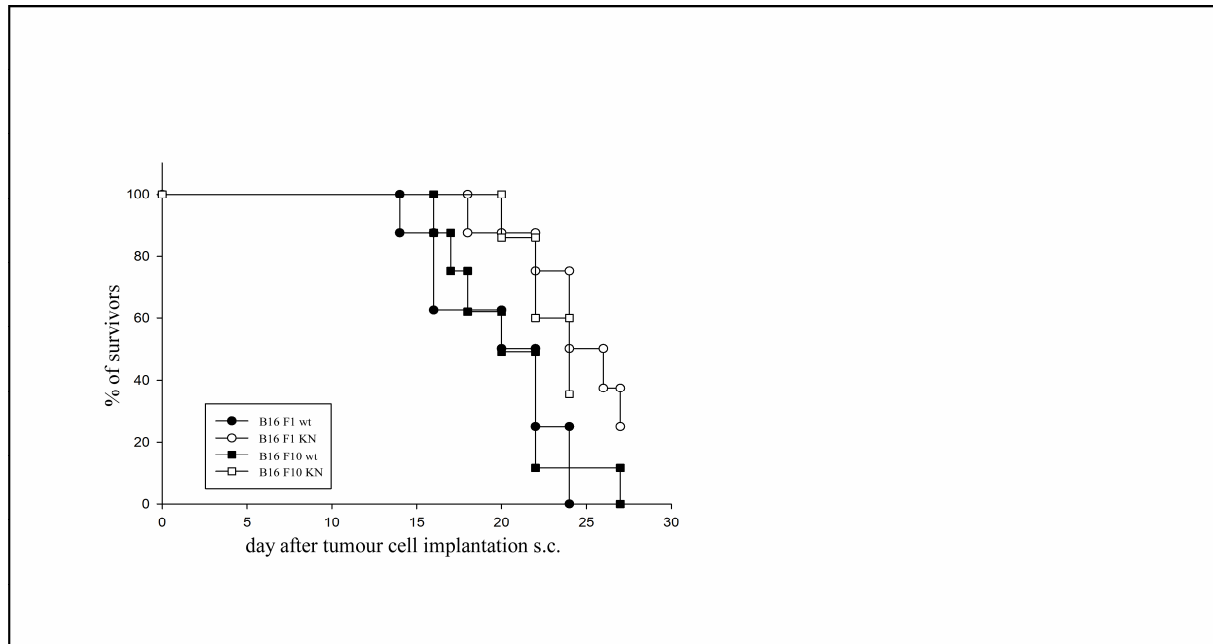


**Figure 17:** Survival of wild-type mice after subcutaneous (s.c.) injection with B16 mouse melanoma cells. Wild-type mice injected with B16 F1 wt and B16 F10 wt cells died earlier than mice injected with the corresponding knock-down (KN) cell lines. (B16 F1 wt n=8, B16 F1 KN n=7, B16 F10 wt n=8, B16 F10 KN n=9)(Injection of cells and further analysis was done by Nikola Baschuk).

To determine whether the reduced diameter of tumours from B16 mouse melanoma FAN knock-down cells was due to a reduced proliferation rate in these cells, proliferation assays were performed.  $10^5$  cells per cell line were seeded on 6 well plates and the number of viable cells after 24 hours, 48 hours and 72 hours was determined. As expected, the FAN knock-down cell lines of both, B16 F1 and B16 F10 mouse melanoma cells exhibited a reduced proliferation rate (Fig. 18). After 24 hours there was only a slight difference in the number of viable cells between wild-type/scrambled and knock-down cells, but after 72 hours the number of viable cells was significantly lower in the FAN knock-down cell lines. On average there were 2.5 Mio B16 F1 wild-type cells and only 1.7 Mio B16 F1 L6M5 and B16 F1 L6E3 cells. In the B16 F10 cell lines on average there were 3.5 Mio viable wild-type cells after 72 hours and only 2.3 Mio B16 F10 L8M2 and 2.7 Mio B16 F10 L8E4 cells (Fig. 18).

## 4. Results

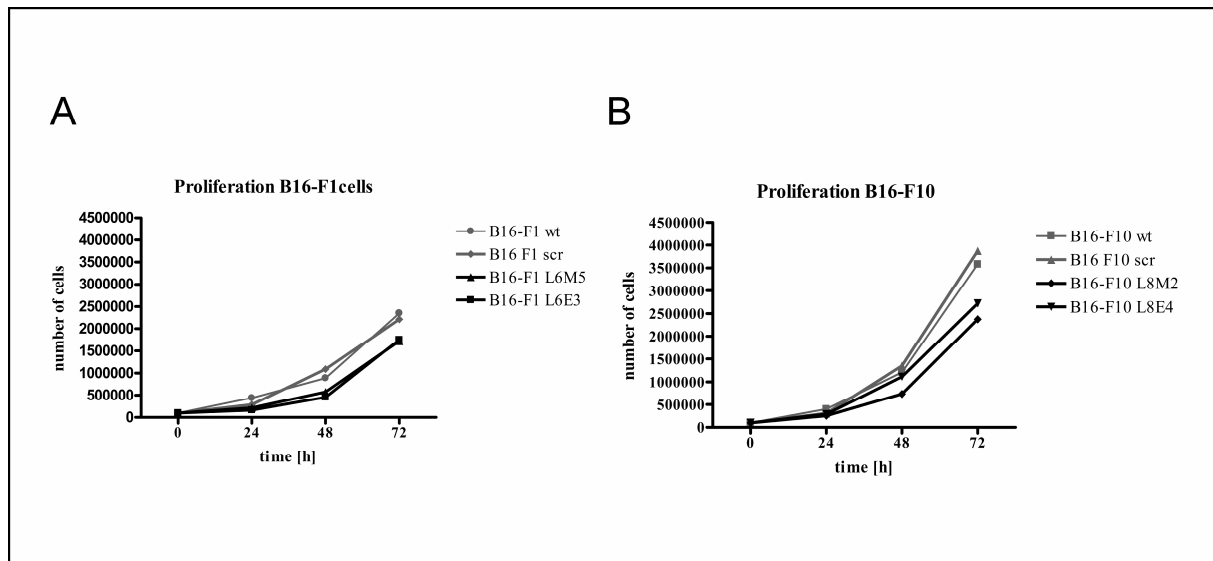


**Figure 18:** A) Proliferation assay of B16 F1 mouse melanoma cell lines. FAN knockdown cell lines (black lines) proliferate more slowly compared to B16 F1 wt and B16 F1 scrambled cells (grey lines). B) Proliferation assay of B16 F10 mouse melanoma cell lines. FAN knockdown cell lines (black lines) proliferate more slowly compared to B16 F10 wt and B16 F10 scrambled cells (grey lines).

To test whether B16 mouse melanoma cells lacking FAN also display a reduction of metastasis *in vivo* in addition to reduced tumour growth, different B16 mouse melanoma cell lines were injected in the tail vein of wild-type mice. The lungs of injected mice were dissected 19 days after injection to see if metastasis had developed (Fig 19). Mice injected with B16 F1 wild-type cells exhibited some metastasis in the lungs after 19 days while in mice injected with B16 F1 FAN knock-down cells metastasis could never be detected. B16 F10 wild-type cells produced more metastasis in the lungs compared to B16 F1 wt cells. This was expected because the B16 F10 cells are much more aggressive than the B16 F1 wt cells which is a less aggressive cancer cell line. Nevertheless, even these highly aggressive B16 F10 mouse melanoma cells did not form metastasis when FAN is down-regulated (Fig. 19)

4. Results

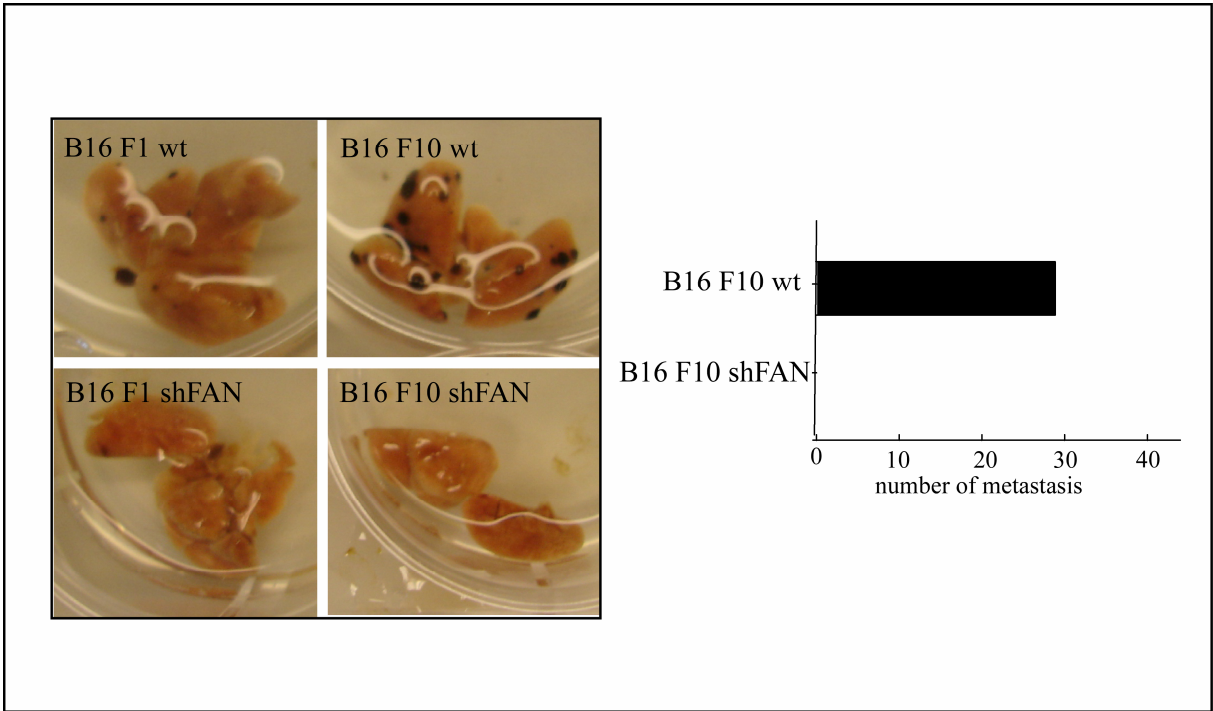


**Figure 19:** Dissected lungs of mice injected with the different cell lines. B16 F1 wt and B16 F10 wt cells form metastasis in the lungs while mice injected with the knock-down cell lines do not exhibit any metastasis in the lungs (n=6/cell line) (Injection of cells and statistical analysis were done by Nikola Baschuk).

### 5. Discussion

Accumulating evidence suggests that FAN might be involved in the motility of cells (Haubert et al. 2007; Montfort et al. 2009). It was recently reported that FAN links the TNF receptor I to the actin cytoskeleton and is essentially involved in filopodia formation in MEF cells (Haubert et al. 2007). Furthermore, recruitment of neutrophils into the peritoneal cavity was reduced by more than 50 % in FAN-deficient mice (Montfort et al. 2009). Although these findings suggest a role for FAN in cell motility, formal proof was missing. The use of a transgenic zebrafish line with fluorescently-tagged leukocytes and the translucency of the embryos have now allowed to demonstrate *in vivo* the essential role of FAN in the navigation of leukocytes towards chemotactic cues emanating from tissue-damage or infection. Furthermore, zebrafish larvae provide an ideal miniature model of the human wound migratory cell response, because only 20 to 30 leukocytes are drawn to a wound, which can be tracked individually by live imaging with fine spatial and temporal precision.

In this work, a single FAN homolog in the zebrafish genome, located on chromosome 7, was identified, which encodes for a protein with 911 amino acids and is expressed throughout all analysed stages of development until day 6. Sequence comparison between mouse and zebrafish FAN revealed a total homology of 70% and a consensus homology of 78.5%, suggesting an evolutionary conserved role in cellular processes. FAN was successfully down-regulated by morpholinos injected into zebrafish embryos at the one- to two-cell stage. One important observation indicated that upon injury at the tail fin the number of leukocytes that assemble at the site of injury was markedly reduced in FAN-MO injected embryos compared to wild-type or control embryos left untreated. Tracking of individual leukocytes revealed that fewer leukocytes arrive at the site of injury. This was due to an impaired directionality of leukocytes in FAN-morphants. The average speed, however, was not affected.

The rapid recruitment of macrophages and neutrophils is essential to coordinate wound closure. Recently, Niethammer and co-workers reported that a gradient of hydrogen peroxide is an initial chemoattractant generated by a wounded tail fin in zebrafish larvae (Niethammer et al. 2009). In fact, a myriad of signalling molecules originate from a wound such as chemokines that attract leukocytes to a wound site. Notably TNF is released upon injury or infection and leukocytes start to move towards the site of TNF (Sieger et al. 2009), suggesting

## 5. Discussion

---

that FAN action in chemotactic responses is triggered by TNF. This is consistent with previous observation that FAN-deficient murine embryonic fibroblasts (MEFs) display an impaired Golgi apparatus reorientation in a scratch-wound test (Haubert et al. 2007). This reorientation of the Golgi apparatus is independent of chemokines suggesting that impaired TNF/FAN signalling is responsible for this defect. TNF is known to have a major function in the initiation and amplification of the inflammatory response by inducing the expression of chemotactic cytokines (chemokines) that are responsible for the migration of several immune cells such as macrophages (Torrente et al. 2003). Because of its chemokine inducing capacity TNF has been sensed as an indirect activator of chemotaxis rather than itself being a direct activator of oriented migration. In lieu of any evidence FAN binds to any known chemokine receptor, the results of this work suggest that TNF via FAN is directly involved in ordered migratory responses.

To deal with the question how FAN might regulate the navigational capacity of leukocytes it is instructive to consider the morphological features of the cellular chemotactic response. Directional cues induce pseudopodia oriented towards the gradient, which includes selective retraction, oriented extension and suppression of *de novo* pseudopodia formation (Van Haastert 2010). To move in the direction of a gradient, leukocytes must form many pseudopodia at the site of the cell that is facing the gradient. In this respect, it is important to note that leukocytes from FAN-deficient embryos protrude pseudopodia in all directions instead of having one clear leading edge. Leukocytes in FAN-deficient zebrafish embryos more often form pseudopodia at the “wrong” location resulting in a loss of directionality. In addition, leukocytes from FAN-MO injected embryos exhibit a delayed movement towards the wound, which is probably also caused by multilateral protrusions observed before they begin to move.

As to the molecular mechanisms regulating chemotaxis, studies in *Dictyostelium* have implicated many signalling pathways including the phosphoinositide 3-kinase (PI3K) pathway activating AKT, the TorC2 pathway activating PKB1, a soluble guanylyl cyclase (sGC) that is activated at the leading edge and produces cGMP, and PLA2 that has an unknown mechanism (Bosgraaf et al. 2009b; Bosgraaf et al. 2009a). FAN signalling pathways may regulate pseudopodia formation in several ways. The observed defect in cell polarization and initiation of directed movement suggests problems in the cytoskeletal reorganization upon gradient sensing. The Rho family of small GTPases is known to play a central role in gradient

## 5. Discussion

---

sensing and cell polarization. Inhibition of the small GTPase Cdc42 by overexpression of dominant-negative mutants in neutrophils produces cells that have an irregular front and frequently form multiple leading edges. Cells with impaired Cdc42 signalling are unable to perform chemotaxis, even though cell motility appears intact, which suggests that Cdc42 is required for gradient sensing (reviewed by Charest and Flirtel 2007). Indeed, FAN mediates the TNF-induced modulation of the actin cytoskeleton through Cdc42 and VASP, which promotes F-actin bundling required for plasma membrane protrusions (Haubert et al. 2007). The loss of directionality in FAN knock-down leukocytes is assumed to be due to impaired Cdc42 signalling. Cdc42 mediates filopodia formation but it also influences Rac signalling, through PAK1 activation, which in turn mediates lamellipodia formation (Nobes and Hall 1995; Nobes and Hall 1999). The formation of lamellipodia itself is not disturbed in FAN morphant embryos but in contrast to wild-type embryos they protrude lamellipodia in every direction instead of having one clear leading edge. This could be due to impaired reorganisation of the golgi apparatus which is mediated by Cdc42 or because the Cdc42 signalling to Rac is disturbed. Furthermore, Cdc42 mediates filopodia formation. FAN deficient MEF cells display reduced filopodia formation (Haubert et al. 2007). Filopodia are not directly involved in migration, they are structures for environment sensing. The reduction of filopodia formation in FAN deficient MEF cells could result in a loss of the sensing capacity of these cells and this could lead to the loss of directionality. This is in line with the knock-down results of the Cdc42 effector molecule WASP. Cvejic et al. could show that WASP knockdown macrophages have a reduced chemotactic index resulting in a reduced number of macrophages reaching the site of injury (Cvejic et al. 2008).

Interestingly, FAN mediates the activation of neutral sphingomyelinase (nSMase) by TNF (Adam-Klages et al. 1996; Adam et al. 1996), which has been recently shown to involve the polycomb group protein EED (Philipp et al. 2010). NSMase is a type C phospholipase like phospholipase PLA2 that plays a crucial role for pseudopodia splitting and directional migration in *Dictyostelium* (Bosgraaf et al. 2009b; Bosgraaf et al. 2009a). Thus, it will be interesting to investigate whether FAN regulates the navigational capacity of leukocytes through neutral sphingomyelinase.

It is important to note that similar navigational defects could be observed after infection of the otic placode with red fluorescent *E.coli*. The reaction of FAN-deficient leukocytes to infection was impaired so that they could not move directly toward the site of infection. Moreover FAN-deficient leukocytes seemed to lose their orientation. Similar defective migratory

## 5. Discussion

---

phenotypes of leukocytes in two different tissues with two different stimuli suggest that FAN plays a general role in chemotaxis.

In addition to the migratory defect of leukocytes in FAN morphant embryos it was revealed that leukocytes from FAN morphant embryos exhibit a reduced bacterial uptake compared to wild-type embryos and therefore pathogen clearance seems to be disturbed in FAN morphant zebrafish embryos. Montfort et al. reported that there is no increased susceptibility to different microorganisms including bacteria and pathogens indicating that FAN is not essential for pathogen clearance. These findings are no caveat to the findings that bacterial uptake in FAN-deficient zebrafish embryos is reduced. To reveal if this reduction in bacterial uptake leads to an increased susceptibility to pathogens long-term observations up to several days instead of only 1.5 hours in zebrafish embryos infected with a fish pathogen are necessary. But even if this observation would reveal that zebrafish embryos are more susceptible to pathogens this could be explained by the fact that Montfort et al. used adult mice for infection studies. Adult mice have an innate and an adaptive immune system while 2 dpf zebrafish embryos only have an innate immune system. It was reported that in accordance with the important role of TNF as a mediator of the innate immune system, an impaired defence against certain intracellular pathogens was observed in TNF-RI and TNF-deficient mice, whereas parameters of the adaptive immune system like CD8<sup>+</sup> T-cell cytotoxicity, mixed lymphocyte response, T-cell-independent B-cell response and most parameters of T-cell-dependent B-cell response remained grossly normal (Marino et al. 1997; Wajant et al. 2003). It is likely that possible defects in the innate immune system in adult FAN knock-out mice can be compensated by the action of the adaptive immune system resulting in a normal immune response while defects in zebrafish embryos at day two can not be compensated by the adaptive immune system as this develops in week 2-3 post fertilisation.

FAN has an impact on actin reorganisation and FAN deficiency leads to a defective leukocyte recruitment to wounds and sites of infection *in vivo*. Another process that requires the reorganisation of the actin cytoskeleton and cell migration is tumour growth and metastasis. To examine whether FAN has also an impact on these processes, stable B16 F1 and B16 F10 mouse melanoma knock-down cell lines were generated. Performance of migration assays revealed that the migration of B16 mouse melanoma FAN knock-down cells is not inducible by TNF stimulation, which is a further hint for the general involvement of FAN in cell migration.

Tumour cell implantation of both, B16 mouse melanoma wild-type and FAN knock-down cells, in the neck of wild-type mice revealed a higher survival rate of mice injected with the B16 mouse melanoma FAN knock-down cell lines. In addition, a reduction in tumour diameter in mice injected with B16 mouse melanoma FAN knock-down cells could be observed (unpublished data, Nikola Baschuk). The reduced diameter of tumours from FAN knock-down cell lines led to the hypothesis that FAN knock-down cells display a reduced proliferation rate. Performance of proliferation assays revealed that FAN knock-down cells indeed display a reduced proliferation rate which is due to a reduced mitosis rate because the viability of FAN knock-down cells was not reduced. It could be observed that FAN deficient cells display less mitotic spindle formation (unpublished data, Catharina Carstens). It has been reported that Cdc42 and Par6/aPKC regulate the orientation of the mitotic spindle to promote symmetric cell divisions in epithelial monolayers (Jaffe et al. 2008). Cdc42 regulates the formation of the central lumen in epithelial morphogenesis. A Cdc42-specific guanine nucleotide exchange factor (GEF), Intersectin 2 (ITSN2), was identified, which localises to the centrosomes and regulates Cdc42 activation during epithelial morphogenesis. Silencing of either Cdc42 or ITSN2 disrupts the correct orientation of the mitotic spindle and normal lumen formation (Rodriguez-Fraticelli et al. 2010). As FAN signals upstream of Cdc42 it is possible that the missing activation of Cdc42 through FAN is also responsible for the reduced proliferation rate in FAN knock-down cells.

Two types of actin-rich adhesions, podosomes and invadopodia establish contact to the substratum and are also involved in the degradation of the extracellular matrix. While podosomes are formed by monocytes, endothelial and smooth muscle cells, invadopodia have mostly been observed in carcinoma cells. Matrix degradation localised at podosomes and invadopodia is thought to contribute to physiological processes, such as monocyte extravasation and tissue transmigration, but also in pathological conditions as cancer metastasis (Linder 2007). Matrix-degrading metalloproteases (MMPs) as well as FAN-GFP localised to invadopodia in B16 mouse melanoma cells. It could be observed that B16 mouse melanoma FAN knock-down cell lines form less invadopodia compared to their wild-type counterparts (unpublished data, Catharina Carstens). Degradation assays of B16 mouse melanoma cells revealed that matrix degradation is reduced in B16 mouse melanoma FAN knock-down cell lines according to the extent of FAN down-regulation. An activity assay of MMPs revealed that in B16 mouse melanoma FAN knock-down cell lines the activity of

## 5. Discussion

---

metalloproteases is reduced and western blot analysis displayed a reduced expression of MT1-MMP in B16 mouse melanoma FAN knock-down cell lines (unpublished data, Catharina Carstens). It was previously reported that the activation of Cdc42 increases the cell surface localisation of MT1-MMP and activation of MMP2. In addition MMP2 and MT1-MMP are specifically up-regulated in response to reorganisation of the actin cytoskeleton and Cdc42 activation (Ispanovic et al. 2008). As FAN is critically involved in the TNF-induced activation of Cdc42 (Haubert et al. 2007), it is likely that FAN deficiency also leads to a decrease in matrix-degradation via reduced MMP activation. To this end, the reduced metastasis observed after tail vein injection of B16 mouse melanoma FAN knock-down cells can be explained by the reduced matrix degradation and in addition to the migratory defect displayed by these cells.

In summary, FAN signals upstream of Cdc42. The activation of Cdc42 through FAN signalling is necessary for many essential processes that require the reorganisation of the actin cytoskeleton like migration, proliferation and matrix degradation. For this purpose it will be interesting to define the molecular mechanisms of Cdc42 activation through FAN signalling.

## 6. References

- Adam-Klages, S., D. Adam, K. Wiegmann, S. Struve, W. Kolanus, J. Schneider-Mergener, and M. Kronke. 1996. FAN, a novel WD-repeat protein, couples the p55 TNF-receptor to neutral sphingomyelinase. *Cell* 86:937-947.
- Adam, D., K. Wiegmann, S. Adam-Klages, A. Ruff, and M. Kronke. 1996. A novel cytoplasmic domain of the p55 tumor necrosis factor receptor initiates the neutral sphingomyelinase pathway. *The Journal of biological chemistry* 271:14617-14622.
- Aggarwal, B.B. 2003. Signalling pathways of the TNF superfamily: a double-edged sword. *Nature reviews* 3:745-756.
- Boldin, M.P., I.L. Mett, and D. Wallach. 1995. A protein related to a proteasomal subunit binds to the intracellular domain of the p55 TNF receptor upstream to its 'death domain'. *FEBS letters* 367:39-44.
- Bosgraaf, L., and P.J. Van Haastert. 2009b. The ordered extension of pseudopodia by amoeboid cells in the absence of external cues. *PLoS one* 4:e5253.
- Bosgraaf, L., and P.J. Van Haastert. 2009a. Navigation of chemotactic cells by parallel signaling to pseudopod persistence and orientation. *PLoS one* 4:e6842.
- Brenner, D.A., M. O'Hara, P. Angel, M. Chojkier, and M. Karin. 1989. Prolonged activation of jun and collagenase genes by tumour necrosis factor-alpha. *Nature* 337:661-663.
- Brucoleri, A., R. Gallucci, D.R. Germolec, P. Blackshear, P. Simeonova, R.G. Thurman, and M.I. Luster. 1997. Induction of early-immediate genes by tumor necrosis factor alpha contribute to liver repair following chemical-induced hepatotoxicity. *Hepatology (Baltimore, Md)* 25:133-141.
- Charest, P.G., and R.A. Firtel. 2007. Big roles for small GTPases in the control of directed cell movement. *The Biochemical journal* 401:377-390.
- Chen, G., and D.V. Goeddel. 2002. TNF-R1 signaling: a beautiful pathway. *Science (New York, N.Y)* 296:1634-1635.
- Choo-Kang, B.S., S. Hutchison, M.B. Nickdel, R.V. Bundick, A.J. Leishman, J.M. Brewer, I.B. McInnes, and P. Garside. 2005. TNF-blocking therapies: an alternative mode of action? *Trends in immunology* 26:518-522.
- Cvejic, A., C. Hall, M. Bak-Maier, M.V. Flores, P. Crosier, M.J. Redd, and P. Martin. 2008. Analysis of WASp function during the wound inflammatory response--live-imaging studies in zebrafish larvae. *Journal of cell science* 121:3196-3206.
- Dahm, R., and R. Geisler. 2006. Learning from small fry: the zebrafish as a genetic model organism for aquaculture fish species. *Marine biotechnology (New York, N.Y)* 8:329-345.
- Diehl, A.M., M. Yin, J. Fleckenstein, S.Q. Yang, H.Z. Lin, D.A. Brenner, J. Westwick, G. Bagby, and S. Nelson. 1994. Tumor necrosis factor-alpha induces c-jun during the regenerative response to liver injury. *The American journal of physiology* 267:G552-561.
- Feng, Y., C. Santoriello, M. Mione, A. Hurlstone, and P. Martin. 2010. Live imaging of innate immune cell sensing of transformed cells in zebrafish larvae: parallels between tumor initiation and wound inflammation. *PLoS biology* 8:e1000562.
- Hanazawa, S., A. Takeshita, S. Amano, T. Semba, T. Nirazuka, H. Katoh, and S. Kitano. 1993. Tumor necrosis factor-alpha induces expression of monocyte chemoattractant JE via fos and jun genes in clonal osteoblastic MC3T3-E1 cells. *The Journal of biological chemistry* 268:9526-9532.

## 6. References

---

- Haubert, D., N. Gharib, F. Rivero, K. Wiegmann, M. Hosel, M. Kronke, and H. Kashkar. 2007. PtdIns(4,5)P-restricted plasma membrane localization of FAN is involved in TNF-induced actin reorganization. *The EMBO journal* 26:3308-3321.
- Hehlgans, T., and D.N. Mannel. 2002. The TNF-TNF receptor system. *Biological chemistry* 383:1581-1585.
- Ispanovic, E., D. Serio, and T.L. Haas. 2008. Cdc42 and RhoA have opposing roles in regulating membrane type 1-matrix metalloproteinase localization and matrix metalloproteinase-2 activation. *Am J Physiol Cell Physiol* 295:C600-610.
- Jaffe, A.B., N. Kaji, J. Durgan, and A. Hall. 2008. Cdc42 controls spindle orientation to position the apical surface during epithelial morphogenesis. *The Journal of cell biology* 183:625-633.
- Jogl, G., Y. Shen, D. Gebauer, J. Li, K. Wiegmann, H. Kashkar, M. Kronke, and L. Tong. 2002. Crystal structure of the BEACH domain reveals an unusual fold and extensive association with a novel PH domain. *The EMBO journal* 21:4785-4795.
- Kreder, D., O. Krut, S. Adam-Klages, K. Wiegmann, G. Scherer, T. Plitz, J.M. Jensen, E. Proksch, J. Steinmann, K. Pfeffer, and M. Kronke. 1999. Impaired neutral sphingomyelinase activation and cutaneous barrier repair in FAN-deficient mice. *The EMBO journal* 18:2472-2479.
- Linder, S. 2007. The matrix corroded: podosomes and invadopodia in extracellular matrix degradation. *Trends in cell biology* 17:107-117.
- Locksley, R.M., N. Killeen, and M.J. Lenardo. 2001. The TNF and TNF receptor superfamilies: integrating mammalian biology. *Cell* 104:487-501.
- Malagarie-Cazenave, S., B. Segui, S. Leveque, V. Garcia, S. Carpentier, M.F. Altie, A. Brouchet, V. Gouaze, N. Andrieu-Abadie, Y. Barreira, H. Benoist, and T. Levade. 2004. Role of FAN in tumor necrosis factor-alpha and lipopolysaccharide-induced interleukin-6 secretion and lethality in D-galactosamine-sensitized mice. *The Journal of biological chemistry* 279:18648-18655.
- Marino, M.W., A. Dunn, D. Grail, M. Inglese, Y. Noguchi, E. Richards, A. Jungbluth, H. Wada, M. Moore, B. Williamson, S. Basu, and L.J. Old. 1997. Characterization of tumor necrosis factor-deficient mice. *Proceedings of the National Academy of Sciences of the United States of America* 94:8093-8098.
- Micheau, O., and J. Tschopp. 2003. Induction of TNF receptor I-mediated apoptosis via two sequential signaling complexes. *Cell* 114:181-190.
- Min, W., and J.S. Pober. 1997. TNF initiates E-selectin transcription in human endothelial cells through parallel TRAF-NF-kappa B and TRAF-RAC/CDC42-JNK-c-Jun/ATF2 pathways. *J Immunol* 159:3508-3518.
- Montfort, A., B. de Badts, V. Douin-Echinard, P.G. Martin, J. Iacovoni, C. Nevoit, N. Therville, V. Garcia, M.A. Bertrand, M.H. Bessieres, M.C. Trombe, T. Levade, H. Benoist, and B. Segui. 2009. FAN stimulates TNF(alpha)-induced gene expression, leukocyte recruitment, and humoral response. *J Immunol* 183:5369-5378.
- Mullins, M.C., M. Hammerschmidt, P. Haffter, and C. Nusslein-Volhard. 1994. Large-scale mutagenesis in the zebrafish: in search of genes controlling development in a vertebrate. *Curr Biol* 4:189-202.
- Mullis, K., F. Faloona, S. Scharf, R. Saiki, G. Horn, and H. Erlich. 1986. Specific enzymatic amplification of DNA in vitro: the polymerase chain reaction. *Cold Spring Harbor symposia on quantitative biology* 51 Pt 1:263-273.
- Nicholson-Dykstra, S., H.N. Higgs, and E.S. Harris. 2005. Actin dynamics: growth from dendritic branches. *Curr Biol* 15:R346-357.
- Niethammer, P., C. Grabher, A.T. Look, and T.J. Mitchison. 2009. A tissue-scale gradient of hydrogen peroxide mediates rapid wound detection in zebrafish. *Nature* 459:996-999.

## 6. References

---

- Nobes, C.D., and A. Hall. 1995. Rho, rac, and cdc42 GTPases regulate the assembly of multimolecular focal complexes associated with actin stress fibers, lamellipodia, and filopodia. *Cell* 81:53-62.
- Nobes, C.D., and A. Hall. 1999. Rho GTPases control polarity, protrusion, and adhesion during cell movement. *The Journal of cell biology* 144:1235-1244.
- O'Brien, N.W., N.M. Gellings, M. Guo, S.B. Barlow, C.C. Glembotski, and R.A. Sabbadini. 2003. Factor associated with neutral sphingomyelinase activation and its role in cardiac cell death. *Circulation research* 92:589-591.
- Peri, F., and C. Nusslein-Volhard. 2008. Live imaging of neuronal degradation by microglia reveals a role for v0-ATPase a1 in phagosomal fusion in vivo. *Cell* 133:916-927.
- Perkins, N.D. 2000. The Rel/NF-kappa B family: friend and foe. *Trends in biochemical sciences* 25:434-440.
- Pfeffer, K., T. Matsuyama, T.M. Kundig, A. Wakeham, K. Kishihara, A. Shahinian, K. Wiegmann, P.S. Ohashi, M. Kronke, and T.W. Mak. 1993. Mice deficient for the 55 kd tumor necrosis factor receptor are resistant to endotoxic shock, yet succumb to L. monocytogenes infection. *Cell* 73:457-467.
- Philipp, S., M. Puchert, S. Adam-Klages, V. Tchikov, S. Winoto-Morbach, S. Mathieu, A. Deerberg, L. Kolker, N. Marchesini, D. Kabelitz, Y.A. Hannun, S. Schutze, and D. Adam. 2010. The Polycomb group protein EED couples TNF receptor 1 to neutral sphingomyelinase. *Proceedings of the National Academy of Sciences of the United States of America* 107:1112-1117.
- Pollard, T.D., and G.G. Borisy. 2003. Cellular motility driven by assembly and disassembly of actin filaments. *Cell* 112:453-465.
- Renshaw, S.A., C.A. Loynes, D.M. Trushell, S. Elworthy, P.W. Ingham, and M.K. Whyte. 2006. A transgenic zebrafish model of neutrophilic inflammation. *Blood* 108:3976-3978.
- Ridley, A.J., M.A. Schwartz, K. Burridge, R.A. Firtel, M.H. Ginsberg, G. Borisy, J.T. Parsons, and A.R. Horwitz. 2003. Cell migration: integrating signals from front to back. *Science (New York, N.Y)* 302:1704-1709.
- Rodriguez-Fraticelli, A.E., S. Vergarajauregui, D.J. Eastburn, A. Datta, M.A. Alonso, K. Mostov, and F. Martin-Belmonte. 2010. The Cdc42 GEF Intersectin 2 controls mitotic spindle orientation to form the lumen during epithelial morphogenesis. *The Journal of cell biology* 189:725-738.
- Sambrook, J., Fritsch, E.F. & Maniatis, T. 1989. *Molecular Cloning - A Laboratory Manual*, 2nd Edition.
- Schulte-Merker, S., Ho, R. K., Herrmann, B. G. and Nusslein-Volhard, C. 1992. The protein product of the zebrafish homologue of the mouse T gene is expressed in nuclei of the germ ring and the notochord of the early embryo. *Development* 116, 1021-32.
- Segui, B., N. Andrieu-Abadie, S. Adam-Klages, O. Meilhac, D. Kreder, V. Garcia, A.P. Bruno, J.P. Jaffrezou, R. Salvayre, M. Kronke, and T. Levade. 1999. CD40 signals apoptosis through FAN-regulated activation of the sphingomyelin-ceramide pathway. *The Journal of biological chemistry* 274:37251-37258.
- Segui, B., O. Cuvillier, S. Adam-Klages, V. Garcia, S. Malagarie-Cazenave, S. Leveque, S. Caspar-Bauguil, J. Coudert, R. Salvayre, M. Kronke, and T. Levade. 2001. Involvement of FAN in TNF-induced apoptosis. *The Journal of clinical investigation* 108:143-151.
- Sieger, D., C. Moritz, T. Ziegenhals, , S. Prykhozhij, F. Peri. Long range Ca<sup>2+</sup> waves transmit brain damage signals to microglia *Developmental Cell* in press

## 6. References

---

- Sieger, D., C. Stein, D. Neifer, A.M. van der Sar, and M. Leptin. 2009. The role of gamma interferon in innate immunity in the zebrafish embryo. *Disease models & mechanisms* 2:571-581.
- Tautz, D., and C. Pfeifle. 1989. A non-radioactive in situ hybridization method for the localization of specific RNAs in *Drosophila* embryos reveals translational control of the segmentation gene hunchback. *Chromosoma* 98:81-85.
- Tcherkasowa, A.E., S. Adam-Klages, M.L. Kruse, K. Wiegmann, S. Mathieu, W. Kolanus, M. Kronke, and D. Adam. 2002. Interaction with factor associated with neutral sphingomyelinase activation, a WD motif-containing protein, identifies receptor for activated C-kinase 1 as a novel component of the signaling pathways of the p55 TNF receptor. *J Immunol* 169:5161-5170.
- Torrente, Y., E. El Fahime, N.J. Caron, R. Del Bo, M. Belicchi, F. Pisati, J.P. Tremblay, and N. Bresolin. 2003. Tumor necrosis factor-alpha (TNF-alpha) stimulates chemotactic response in mouse myogenic cells. *Cell transplantation* 12:91-100.
- van der Sar, A.M., R.J. Musters, F.J. van Eeden, B.J. Appelmelk, C.M. Vandenbroucke-Grauls, and W. Bitter. 2003. Zebrafish embryos as a model host for the real time analysis of *Salmonella typhimurium* infections. *Cellular microbiology* 5:601-611.
- Van Haastert, P.J. 2010. Chemotaxis: insights from the extending pseudopod. *Journal of cell science* 123:3031-3037.
- Vandenabeele, P., W. Declercq, R. Beyaert, and W. Fiers. 1995. Two tumour necrosis factor receptors: structure and function. *Trends in cell biology* 5:392-399.
- Wajant, H., K. Pfizenmaier, and P. Scheurich. 2003. Tumor necrosis factor signaling. *Cell death and differentiation* 10:45-65.
- Werneburg, N., M.E. Guicciardi, X.M. Yin, and G.J. Gores. 2004. TNF-alpha-mediated lysosomal permeabilization is FAN and caspase 8/Bid dependent. *American journal of physiology* 287:G436-443.
- Westerfield, M. 1995. The zebrafish book. Eugene, OR: University of Oregon Press.,
- Wiegmann, K., S. Schutze, E. Kampen, A. Himmler, T. Machleidt, and M. Kronke. 1992. Human 55-kDa receptor for tumor necrosis factor coupled to signal transduction cascades. *The Journal of biological chemistry* 267:17997-18001.
- Wigler, M., A. Pellicer, S. Silverstein, and R. Axel. 1978. Biochemical transfer of single-copy eucaryotic genes using total cellular DNA as donor. *Cell* 14:725-731.
- Winder, S.J., and K.R. Ayscough. 2005. Actin-binding proteins. *Journal of cell science* 118:651-654.
- Yang, J., Y. Lin, Z. Guo, J. Cheng, J. Huang, L. Deng, W. Liao, Z. Chen, Z. Liu, and B. Su. 2001. The essential role of MEKK3 in TNF-induced NF-kappaB activation. *Nature immunology* 2:620-624.
- Zhang, Y., X.T. Bai, K.Y. Zhu, Y. Jin, M. Deng, H.Y. Le, Y.F. Fu, Y. Chen, J. Zhu, A.T. Look, J. Kanki, Z. Chen, S.J. Chen, and T.X. Liu. 2008. In vivo interstitial migration of primitive macrophages mediated by JNK-matrix metalloproteinase 13 signaling in response to acute injury. *J Immunol* 181:2155-2164.

## **Erklärung**

Ich versichere, dass ich die von mir vorgelegte Dissertation selbständig angefertigt, die benutzten Quellen und Hilfsmittel vollständig angegeben und die Stellen der Arbeit – einschließlich Tabellen, Karten und Abbildungen –, die anderen Werken im Wortlaut oder dem Sinn nach entnommen sind, in jedem Einzelfall als Entlehnung kenntlich gemacht habe; dass diese Dissertation noch keiner anderen Fakultät oder Universität zur Prüfung vorgelegen hat; dass sie – abgesehen von unten angegebenen Teilpublikationen – noch nicht veröffentlicht worden ist sowie, dass ich eine solche Veröffentlichung vor Abschluss des Promotionsverfahrens nicht vornehmen werde. Die Bestimmungen dieser Promotionsordnung sind mir bekannt. Die von mir vorgelegte Dissertation ist von Prof. Jonathan Howard und Prof. Dr. Martin Krönke betreut worden.

Auszüge dieser Arbeit werden voraussichtlich in Kürze publiziert. Teile der folgenden Publikation entsprechen dem Kapitel 4.1 dieser Arbeit.

**Alexandra Böcke, Dirk Sieger, Cristian Dan Neacsu, Hamid Kashkar and Martin Krönke (2012)** FAN mediates navigational capacity of leukocytes responding to wounds and infection: live imaging studies in zebrafish larvae. *Journal of Immunology* submitted.

## **Declaration of collaborators contributions**

The diverse input of several people has improved the quality of this work. Their contribution is acknowledged below.

The zebrafish experiments were done in collaboration with Dr. Dirk Sieger (EMBL Heidelberg).

The injection of B16 mouse melanoma cells into mice and the statistical analysis of these experiments were done by Nikola Baschuk.

## **Danksagungen**

Ich möchte mich bei Prof. Martin Krönke bedanken für die Möglichkeit, meine Doktorarbeit an seinem Institut anfertigen zu können und die Betreuung meiner Arbeit. Des Weiteren möchte ich mich auch bei Prof. Jonathan Howard für die Betreuung meiner Doktorarbeit von Seiten der Mathematisch-Naturwissenschaftlichen Fakultät bedanken.

Mein ganz besonderer Dank gilt Dirk Sieger. Zum Einen möchte ich mich für die hervorragende fachliche Unterstützung meines Projektes bedanken, zum Anderen für die persönliche Unterstützung.

Danke auch an alle Arbeitskollegen, insbesondere Catharina Carstens für die gute Zusammenarbeit an unserem gemeinsamen Projekt.

Ausserdem möchte ich mich bei meinen Eltern bedanken die mir dieses Studium ermöglicht haben.

## **Lebenslauf**

**Name:** Böcke  
**Vorname:** Alexandra  
**Adresse:** Weidenweg 5  
51491 Overath  
**Geburtsdatum:** 21.01.1982  
**Geburtsort:** Bergisch Gladbach  
**Nationalität:** deutsch  
**Familienstand:** ledig  
**Studium:** seit Jan. 2008: Beginn der Promotion bei Prof. M. Krönke am Institut für medizinische Mikrobiologie, Immunologie und Hygiene – Titel: FAN mediates navigational capacity in leukocytes and tumour cells  
  
2001- 2007 Biologie Universität zu Köln  
Abschluss: Diplom  
  
**Schullaufbahn:** 1992-2001 Paul-Klee Gymnasium Overath  
Abschluss: Abitur  
1988-1992 Gemeinschaftsgrundschule Overath

Köln, den 14.04.2012

Alexandra Böcke